AWARD NUMBER: W81XWH-18-1-0700

TITLE: HIOC Derivatives for the Treatment of Trauma-Induced Vision Loss

PRINCIPAL INVESTIGATOR: Paul Michael Iuvone, Ph.D.

CONTRACTING ORGANIZATION: Emory University, Atlanta, GA

REPORT DATE: January 2023

TYPE OF REPORT: Final

PREPARED FOR: U.S. Army Medical Research and Development Command
Fort Detrick, Maryland 21702-5012

REPORT DOCUMENTATION PAGE

Form Approved
OMB No. 0704-0188

1. REPORT DATE	2. REPORT TYPE	3. DATES COVERED
January 2023	Final	15Sep2018-14Sep2022

4. TITLE AND SUBTITLE

HIOC Derivatives for the Treatment of Trauma-Induced Vision Loss

5a. CONTRACT NUMBER

5b. GRANT NUMBER
W81XWH-18-1-0700

5c. PROGRAM ELEMENT NUMBER

6. AUTHOR(S)
P. Michael Iuvone
Frank E. McDonald

E-Mail: miuvone@emory.edu

5d. PROJECT NUMBER

5e. TASK NUMBER

5f. WORK UNIT NUMBER

7. PERFORMING ORGANIZATION NAME(S) AND ADDRESS(ES)

Emory University
Atlanta, GA 30322

8. PERFORMING ORGANIZATION REPORT NUMBER

9. SPONSORING / MONITORING AGENCY NAME(S) AND ADDRESS(ES)

U.S. Army Medical Research and Development Command
Fort Detrick, Maryland 21702-5012

10. SPONSOR/MONITOR'S ACRONYM(S)

11. SPONSOR/MONITOR'S REPORT NUMBER(S)

12. DISTRIBUTION / AVAILABILITY STATEMENT

Approved for Public Release; Distribution Unlimited

13. SUPPLEMENTARY NOTES

14. ABSTRACT

Pressure waves due to explosions can damage the neurons of the eye and visual centers in the brain, leading to visual function loss. There are currently few treatments for such injuries that can be deployed rapidly in the field to mitigate such damage. We have developed small molecule activators of TrkB, the cognate receptor for brain-derived neurotrophic factor (BDNF), which cross the blood/retina and blood/brain barriers. Based on a preliminary lead compound, *N*-[2-(5-hydroxy-1H-indol-3-yl)ethyl]-2-oxopiperidine-3-carboxamide (HIOC), we synthesized and tested the biological activity of 28 derivatives. At least two analogs have TrkB activation potency that is clearly superior to HIOC. Our best candidate is 2-fluoro-*N*-(2-(5-hydroxy-1H-indol-3-yl)ethyl)nicotinamide (HIFN), which protects against blast-induced loss of visual function in a small animal model, when injected at a maximally effective dose of 30 mg/kg within three hours of trauma. HIFN exhibits no detectable acute or chronic toxicity in treated animals.

15. SUBJECT TERMS
Blast injury, vision loss, therapeutics

16. SECURITY CLASSIFICATION OF:			17. LIMITATION OF ABSTRACT	18. NUMBER OF PAGES	19a. NAME OF RESPONSIBLE PERSON
a. REPORT	b. ABSTRACT	c. THIS PAGE			USAMRDC
Unclassified	Unclassified	Unclassified	Unclassified	44	19b. TELEPHONE NUMBER *(include area code)*

TABLE OF CONTENTS

1. INTRODUCTION: Retinal damage followed by vision loss caused by traumatic blast-related injury, sports injury, or other blunt force trauma to the eye is a serious public health issue, affecting military personnel and the general public. To prevent vision loss from trauma, treatment must be started quickly during a critical period before irreversible neuronal degeneration is initiated. The purpose of the funded research was to develop new pharmaceutical treatments for trauma-induced vision loss that can be administered on the battlefield, in field hospitals, or in ambulances. We specifically developed small molecule therapeutics that can be administered by systemic injection, get into the retina and brain from the blood stream, and protect from trauma-induced vision loss. Starting with a lead compound, HIOC, that was shown to be effective in preventing vision loss caused by blast injury to the eye and brain, we studied the activity of a family of HIOC derivatives that were designed to have superior penetrance into the retina and brain. We assessed the activity of 28 novel structural analogs of HIOC, focusing on TrkB receptor activators in cell studies, followed by *in vivo* studies of 2 analogs in mice to determine the most promising compound from several promising candidates. We conducted preclinical pharmacokinetic and toxicological studies on the best candidate compound, 2-fluoro-*N*-(2-(5-hydroxy-1H-indol-3-yl)ethyl)nicotinamide (HIFN).

2. KEYWORDS: acylation, BDNF, computational modeling, enantioselective synthesis, fluoroaromatic, medicinal chemistry, neuroprotection, optic nerve, pyridine, retina, serotonin, TBI, trauma, TrkB

3. ACCOMPLISHMENTS:

- **What were the major goals of the project?**

The goal of this project was to develop effective, battlefield-deliverable treatments for traumatic blast-related retinal and visual system damage.

Specific Aims:

1. Chemical synthesis of HIOC derivatives (years 1 - 4)
2. Examine the efficacy and potency of HIOC derivatives in activating TrkB and preventing vision loss following ocular trauma (years 1 - 4)
3. Pharmacokinetic and toxicological analysis of HIFN (year 4)

- **What was accomplished under these goals?**

1. Major activities: Co-PI Prof. Frank E. McDonald and postdoctoral associate Dr. Christopher L. Walker designed and synthesized 28 structural analogs of HIOC in quantities sufficient for testing these analogs as TrkB activators, in work conducted by PI P. Michael Iuvone and postdoctoral associate Dr. Shweta Modgil. For a complete catalog of the analogs synthesized, see Appendix 1. Functional assessments included determining the mechanism contributing to the protective effects of our best analog, HIFN, and determining the critical therapeutic time window for HIFN treatment. Preliminary toxicological studies were conducted, analyzing blood chemistry, serum enzymes, and histopathology, assessed by Dr Hans Grossniklaus.

2. Specific objectives: Objectives included a structure-activity relationship scheme for small molecule activators of TrkB and the associated protective effects, preventing vision loss following ocular trauma, by systematic modifications of *N*-acetylserotonin derivatives. Animal studies were conducted with our best analog, HIFN, seeking to remedy vision deficits due to blast overpressure injury to the eye, and establishing the effective treatment timeframe for HIFN treatment after injury. We also investigated if HIFN protective effects were exerted through TrkB activation.

3. Significant results and key outcomes:

3.1. The characterization of the lead compound, HIOC, was completed and published (Dhakal et al., 2021; Appendix 2). The results can be summarized as follows. The effects of blast-induced ocular trauma on retinal and visual function were characterized. We showed that systemic administration of HIOC, a potent small molecule activator of the BDNF/TrkB receptor, preserves visual function in mice exposed to ocular blast injury. HIOC treatment for one week preserves visual function for at least 4 months. HIOC treatment effectively protected vision when the initial dose was administered up to 3 h after blast, but not if the initial treatment was

delayed for 24 h. We provided evidence that the therapeutic effect of HIOC is mediated by activation of BDNF/TrkB receptors. The results indicate that HIOC may be useful for treating ocular blast injury and other forms of traumatic optic neuropathy.

3.2. Dr. Christopher L. Walker established that the chiral center of our lead compound, HIOC, was configurationally unstable, thus ruling out an enantioselective synthesis of HIOC. However, a crystal structure of HIOC showed that this compound preferred a conformation with the carbonyl groups orthogonally oriented, as depicted below.

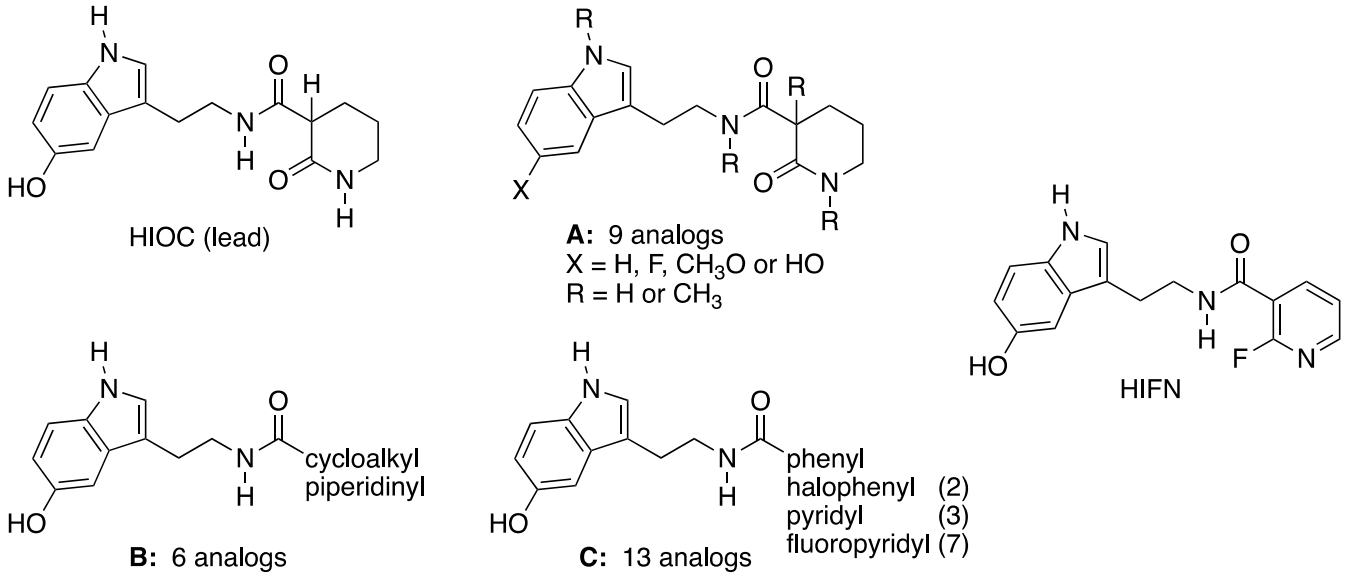

Figure 1. Structure of HIOC, general structures of 28 novel synthetic analogs, and our best compound, HIFN

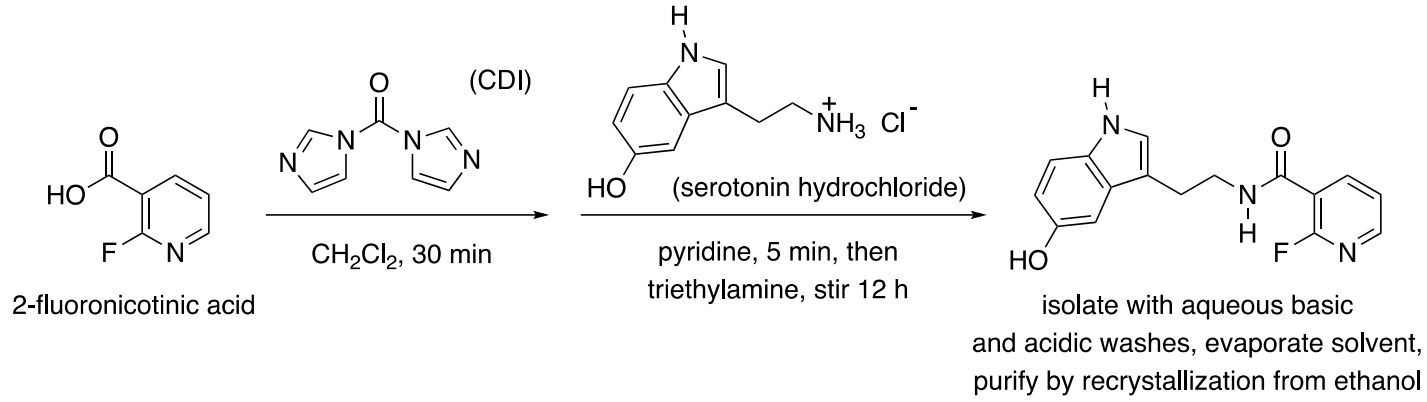

Figure 2. Chemical synthesis of HIFN

Over the course of this project, we optimized and then scaled up the synthesis and purification of HIFN to reliably produce 5 gram batches (**Figure 2**), generating over 30 grams of HIFN in the final year of this project, to support the animal studies described below.

3.3. Biological Characterization of Analogs: *in vitro* screening of analogs

The synthetic analogs of HIOC (**Figure 1**) were tested as TrkB activators in cultured rat cortical neurons and in NIH 3T3 cells expressing human TrkB by measuring the phosphorylation of the receptor by immunoblot analysis. An example of the immunoblot analysis is shown in Figure 3.

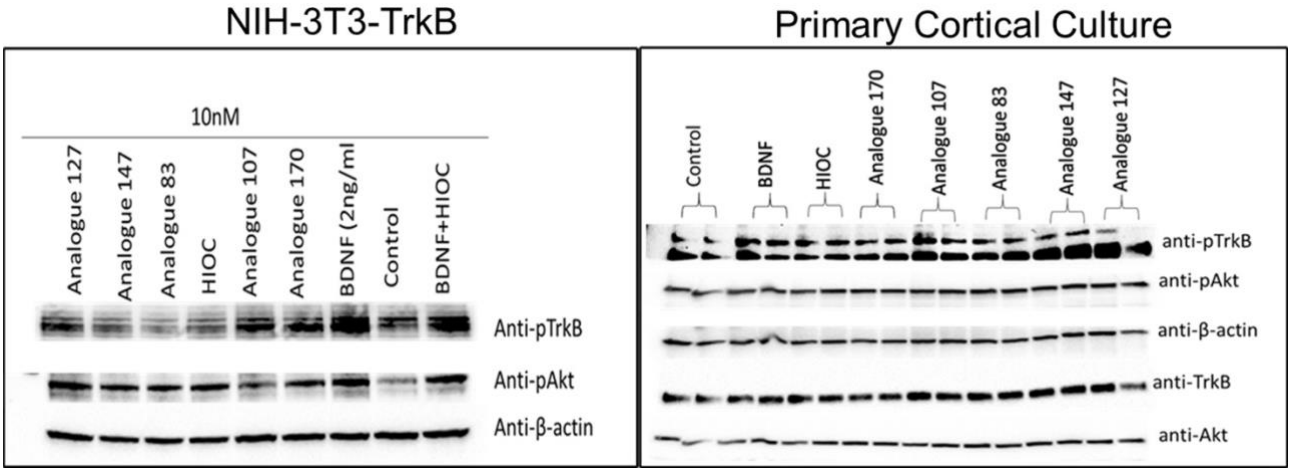

Figure 3

Some of the analogs in class **A** replacing the hydroxyl group with other groups (X = HO, H, F, CH_3O) or selectively replacing hydrogen (R = H) with methyl groups (R = CH_3) showed promising activity, whereas a set of analogs in class **B** with conformationally flexible cycloalkyl and piperidinyl were uniformly less active. Several achiral analogs in class **C** in which the amine of serotonin was acylated with aromatic and heteroaromatic rings were more effective TrkB activators than HIOC. Two of the fluoropyridine analogs were shown to induce TrkB phosphorylation at 10 nM concentration. A crystal structure of HIFN revealed an intramolecular hydrogen bond between the secondary amide N-H and fluorine. This places the electronegative fluorine and nitrogen atoms in a similar but not identical conformation as the electronegative oxygen and nitrogen atoms of HIOC, leaving intact the other structural features of *N*-acetylserotonin (NAS).

A dose-dependent study with our best small molecule analog, 2-**f**luoro-*N*-(2-(5-**h**ydroxy-1*H*-**i**ndol-3-yl)ethyl)**n**icotinamide (HIFN), showed maximal TrkB phosphorylation at 1 nM, comparable to the activity of the neurotrophin TrkB activator BDNF at 2 ng/mL concentration (**Figure 4**).

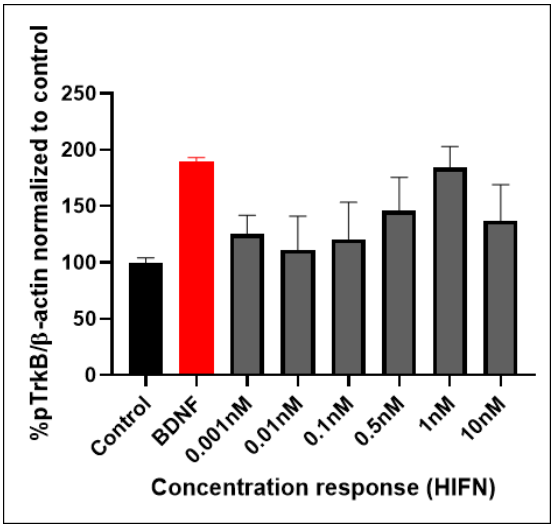

Fig. 4

3.4. Biological Characterization of Analogs: *in vivo* screening of analogs

Our cell culture studies showed that analog 127 and 147 (HIFN) both effectively activate TrkB receptor. Therefore, we aimed to test these compounds in our animal model of blast injury as described earlier. Surprisingly, analog 127 did not provide any protection against vision loss in blast animals. HIFN, however, successfully ameliorated the damage caused by overpressure injury as described below.

3.4.1. HIFN provides stronger protection against visual function deficit than the parent compound HIOC. Male C57BL/6J mice were randomly divided into treatment groups viz., Sham-Vehicle, Blast-Vehicle, Blast-HIOC and Blast-HIFN. In all *in vivo* studies the dose of HIFN and HIOC was 40 mg/kg ip, unless noted otherwise. Mice were treated with vehicle or drugs for 1 week beginning the day of blast exposure. The baseline recordings for contrast sensitivity and visual acuity showed no significant difference between groups (data not shown). Blast exposure significantly altered the visual function outcomes (**Figure 5)**. Contrast sensitivity (CS) deficit was observed at all the timepoints [mixed effect two-way ANOVA group effect {F (3,24) =60.8, p<0.0001};

interaction effect, group × timepoint, {F [6,44] = 3.12, p < 0.05}] (**Figure 5A)**. The decline was seen as early as one week post blast with CS in blast animals reduced to 38.4 ±3.24% (p=0.0001) of sham control animals. It continued to decline (24.3 ± 2.13%, p=0.001) with time, till 7-week post blast (longest timepoint recorded). Treatment with either HIOC (59.6 ± 3.24%, p=0.0017) or HIFN (61.3± 4.50%, p=0.0034) preserved CS providing protection beginning from 1-week post blast compared to vehicle treated animals (38.4±3.24). The decline of contrast sensitivity was significantly less at 5 weeks with HIOC (32.9%, p=0.01) and HIFN (38.9%, p=0.01) compared to vehicle treatment group where CS declined by 66.9%. Moreover, HIFN provided more robust protection in the long term than HIOC. By 7 weeks, HIFN treated animals have 22.3% higher contrast sensitivity than HIOC treatment group (p=0.06).

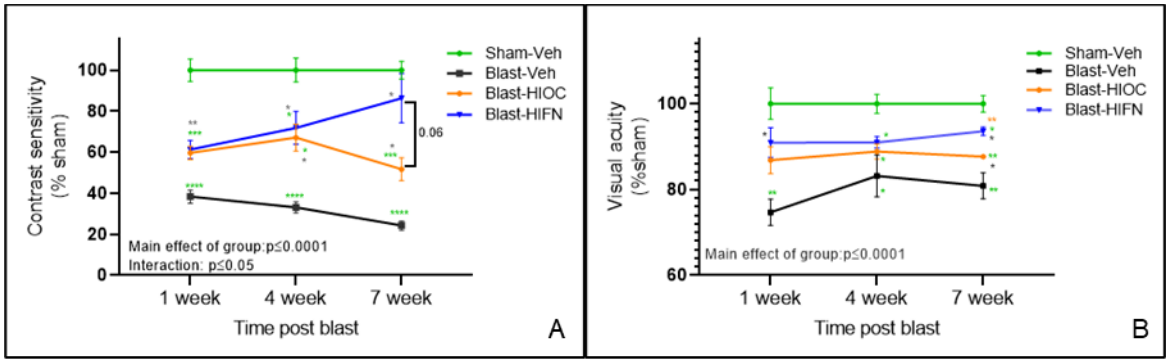

Figure 5. HIFN treatment prevented visual function deficits: Contrast sensitivity (A) and visual acuity (B) at 1,4 and 7-week post blast. Data is presented as % of Sham-Veh±SEM. HIFN rescued visual acuity and contrast sensitivity deficit at all the time points. At 7-weeks visual function is better in HIFN treated animals compared to HIOC.
(A) and (B) *vs Sham-Veh, *vs Blast-Veh, *vs Blast-HIOC; *p≤0.05; ** p≤0.01; ***p≤0.001; ****p≤0.0001; n=6-7per group; REML, Holm Sidak's adjusted p-values used for post-hoc comparisons.

Although compared to CS, visual acuity showed less sensitivity to blast, the spatial frequency deficits were also seen beginning one week post blast exposure. At this time, blast animals were recorded with visual acuity of 0.317±0.013 c/d as compared to 0.424±0.015 c/d in sham control animals (25.23 % decline; p= 0.001). When compared to vehicle group, HIOC and HIFN treatment resulted in better visual acuity preservation [2-way, mixed effect, ANOVA, group effect F (3,24) p=0.001] (**Figure 5B)**. 7-weeks after blast, the visual acuity threshold was 8.28% higher with HIOC [0.340±0.0018 c/d (p=0.06)] and 15.6% with HIFN [0.363±0.0036 c/d (p=0.014)] compared to vehicle treated animals [0.314±0.0074 c/d]. Furthermore, HIFN was significantly better than HIOC in preventing visual acuity deficit (p=0.002) at 7 weeks post blast exposure.

3.4.2. Ocular blast injury selectively affects retinal ganglion cells (RGC): HIFN preserves RGC cell function.

To study the effect of blast on different retinal cell types, we employed electroretinography (ERG) to map the functional outcomes after treatment. A 5-step full field scotopic ERG (–3.0 to 1 log cd. s/m^2) was performed at 3, 6 and 9-week post blast (**Figure 6**). Differences were not observed for any scotopic ERG component across time. **Figure 6A and B** shows a-wave and b-wave amplitudes (mean ± SEM) in different treatment groups at 9-weeks post blast. No significant difference was recorded in photoreceptor and bipolar cell function as analyzed by a-wave [F (3,132) =1.134 p=0.337] and b-wave amplitude [F (3,132) =1.047 p=0.374]. Interestingly, blast animals also did not show any changes in amplitudes. We further isolated oscillatory potential and c wave amplitude from ERGs. OPs are generated from amacrine cell responses on ascending limb of the b-wave while c wave provides retinal pigment cell function. OPs amplitude remained unaltered after the blast exposure [F (3,99) =2.01 p=0.1171]. Similarly, we did not observe any alterations in ERG c-wave amplitudes (p=0.244). These results were in accordance with our previous data where we did not report any significant changes in ERG (Dhakal et al., 2021; Appendix 2).

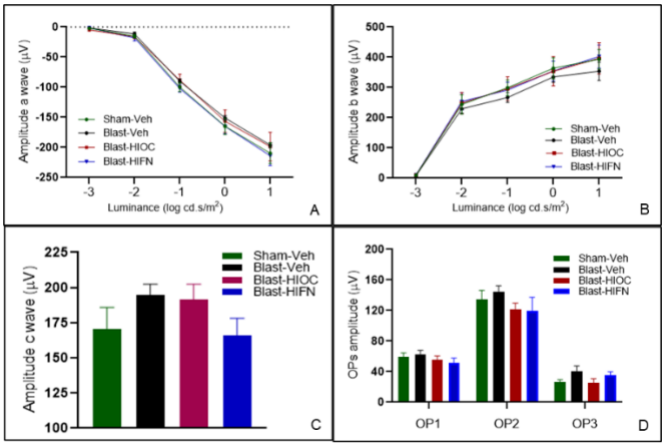

Figure 6. Outer and inner retinal neurons not affected by blast, HIFN, or HIOC. Scotopic ERG was recorded in animals at 9-week post blast. Function of photoreceptors, bipolar cells, retinal pigment epithelial cells and amacrine cells was measured by plotting amplitude a wave (A), amplitude b wave (B), amplitude c wave (C) and oscillatory potentials (D) respectively. No significant difference was found for all the parameters recorded. Data are expressed as mean ± SEM; n=6-8/group

Since none of the outer or inner retinal neurons were affected by blast, we examined the functionality of retinal ganglion cells (RGCs) using pattern ERG (PERG) (**Figure 7**). PERG revealed significant changes in both P1 and N2 wave amplitudes [2-way, mixed model ANOVA, {P1 amplitude group effect F (3,24) =10.6, P=0.0001}; {N2 amplitude, group effect F (3, 65) =10.4, P=0.0001}]. Initial assessment at 2-weeks post blast, did not provide any valuable information of RGC function. No statistically visible changes between sham and blast animals were seen at this time.

However, when these animals were followed for 5 weeks, both P1 [6.11±0.486 (Blast-Veh) vs 9.23±0.372 (Sham-Veh), p=0.051] and N2 wave amplitude [-8.38±0.586 (Blast-Veh) vs –11.9±0.743 (Sham-Veh), p=0.023] were significantly decreased in blast exposed animals. At 5-weeks post blast, P1 {7.63±0.618 (Blast-HIOC) and 8.70±0.726 (Blast-HIFN) vs 6.11±0.486 (Blast-Veh)} and N2 amplitudes {–9.55±0.821 (Blast-HIOC) and –11.3±1.05 (Blast-HIFN) vs –8.38±0.586 (Blast-Veh)} in treatment animals were marginally better than vehicle. A further assessment of RGC function at 8-weeks post blast confirmed continued decline in vehicle treatment group [p=0.01 for P1 amplitude and p=0.007 for N2 amplitude vs Sham-Veh] suggesting slow but progressive decline in RGC cell function. However, at this timepoint both HIFN and HIOC were able to rescue the deficit in RGC cell function and there were significantly higher P1 wave amplitudes in HIOC (p=0.012 vs Blast-Veh) and HIFN (p=0.01 vs Blast-Veh) treated mice. Moreover, there is modest but insignificant improvement in N2 wave amplitude in treatment animals (-11.1±1.01 vs –7.73±0.950, p=0.12 (HIOC vs Veh); -11.2± 0.610 vs –7.73± 0.950, P=0.06 (HIFN vs Veh).

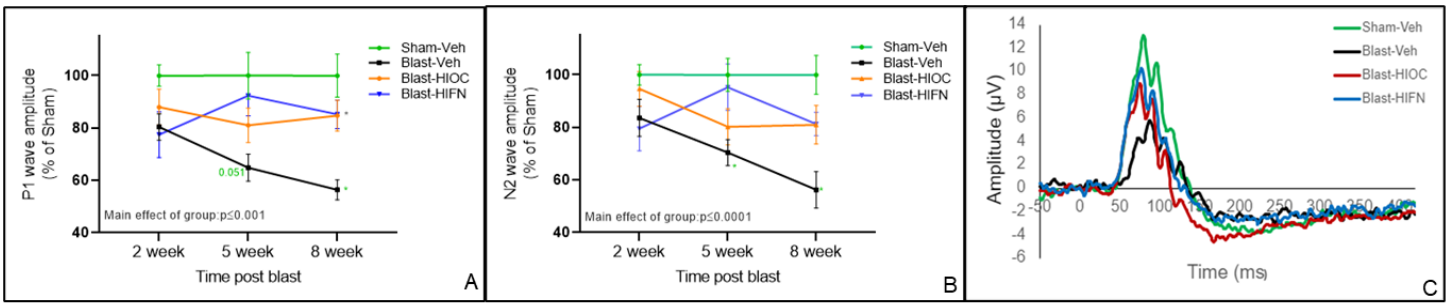

Figure 7. HIFN rescued retinal ganglion cell function decline. Pattern ERG recorded for retinal ganglion cell function assessment at various time post blast. P1 (A) and N2 (B) wave amplitude begin to decline at 5 weeks after blast in vehicle treatment group. HIFN treatment prevented the decline in RGC cell function and preserved the P1 and N2 amplitude at 8-week post blast. C) Representative PERG waveform from each group 8 weeks after blast. (A) and (B) *vs Sham-Veh, *vs Blast-Veh; * p≤0.05; n=5-7per group. Data are expressed as %Sham-Veh ± SEM; REML, Holm Sidak's adjusted p-values used for post-hoc comparisons.

3.4.3. HIFN reduces RGC loss after blast injury

Figure 8 shows representative retinal flatmount staining of RGCs with an antibody to RNA binding protein-multiple splicing (RBPMS), cell-specific marker for RGCs. Regions of interest (ROI) of equal dimension was selected from center (near optic disc), mid and peripheral region of retina (**Figure 8A**), enlarged view of ROI shown in **8B**). Automatic counting of RGCs using RGC plugin (Image J) showed decrease (p=0.07) in RGC cell count per ROI in Blast-Veh (351±9.67) animals compared to the control (379± 5.02). HIFN treatment preserved RGC cell loss when compared to vehicle [382 ±8.17 (HIFN) vs 351±9.67 (Veh), p=0.05] in central retina. However, no difference was observed in RGC cell numbers in mid and peripheral retina regions in animals (Figure 5C).

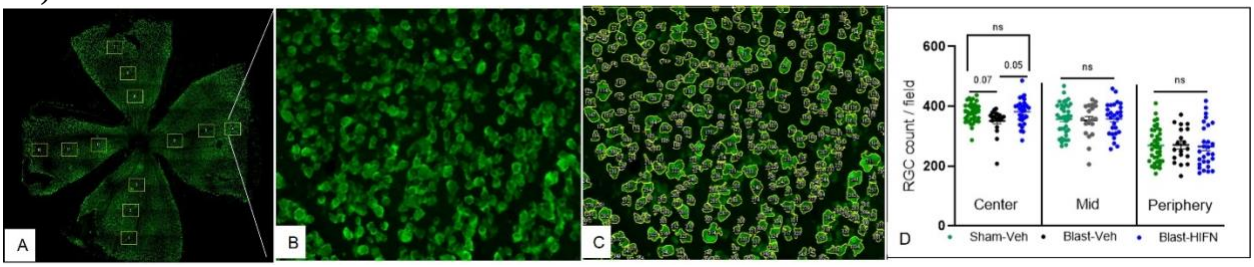

Figure 8. HIFN reduced RGC loss: Retinal flatmounts were stained with RGC-specific marker RBPMS (RNA binding protein multiple splicing). Regions of interest (ROI) were selected from center, mid and peripheral retina (A). Enlarged image of one ROI is shown (B). Cells in ROI were automatically counted using Image J, Simple RGC, plugin (C). RGC cell count decreases in center retina while HIFN treatment prevented the RGC cell loss (D). Data are expressed as Total cells/ ROI (mean ± SEM); n=5-8/group.

3.4.4. HIFN exerts neuroprotective effects through TrkB receptor activation: Prevention of visual function deficit by HIFN was inhibited by ANA-12

We tested the hypothesis that HIFN confers protection against ocular trauma via TrkB receptor activation. ANA-12, a specific TrkB receptor inhibitor was used to inactivate TrkB. Mice were injected with ANA-12 (0.5mg/kg) 2.5 hours before blast exposure. Following blast, they were administered with vehicle or HIFN within 30 minutes. From day 2 to day 7, the ANA-12 pretreatment (2.5 h) followed by vehicle/HIFN treatment was continued. Effects of ANA-12 pretreatment on neuroprotection exerted by HIFN were evaluated.

A significant decline in contrast sensitivity was seen in blast animals compared to control [18.3 ± 0.903 (Sham-Veh) vs 4.83± 0.417 (Blast-Veh); p=0.0001] and HIFN treatment prevented this decline [11.8 ± 0.737 (Blast-HIFN)]. ANA-12 pre-treatment prevented the protective effects of HIFN (**Figure 9A**). At 7-week post blast, HIFN treated animals have significantly better (p=0.02) contrast sensitivity (11.8 ±0.737) than vehicle treated animals (4.83 ± 0.417). This suggests that when animals were pre-treated with ANA-12 prior to vehicle, the contrast sensitivity deficit was not prevented. ANA-12+HIFN group has lower [5.38±0.228 (ANA-12/Blast-HIFN)] contrast sensitivity than HIFN treatment group [11.8 ±0.737 (Veh/Blast-HIFN)] almost reaching a level of significance (p=0.06).

Visual acuity threshold (7-week post blast) revealed the same pattern as contrast sensitivity. Animals treated with HIFN (Veh/Blast-HIFN) have significantly (p=0.017) better visual acuity threshold (0.396±0.008) than vehicle treated group [0.325±0.014 (Veh/Blast-Veh)] (**Figure 9B**). The improvement in visual acuity with HIFN treatment was not seen in animals receiving ANA-12 prior to HIFN (ANA-12/Blast-HIFN). ANA-12+HIFN group was reported with visual acuity (0.326± 0.007) similar to untreated groups [Veh / Blast-Veh group (0.325±0.014)] and ANA-12 / Blast-Veh (0.3280±0.005) while significantly lower (p=0.026) visual acuity than Veh/Blast-HIFN group (0.396±0.008). These results (**Figures 9A and 9B**) support the hypothesis that HIFN acts via TrkB receptor as ANA-12 mitigates the protection exerted by HIFN.

As discussed earlier, HIFN prevented the RGC function deficit induced by traumatic injury, as assessed by PERG. We repeated the experiment with the addition of new groups where animals were treated with ANA-12 prior to HIFN treatment. In parallel with our earlier results, the significant decline in P1 amplitude after blast [5.06±0.432; p=0.01 (Veh/Blast-Veh) and 4.91± 0.251, p=0.004 (ANA-12/Blast-Veh)] compared to Sham (7.80± 0.895) is

prevented by HIFN treatment [7.49± 0.487 (Veh/Sham-HIFN)]. With ANA-12 pretreatment however, this preservation was inhibited. As shown in **Figure 9C**, P1 amplitude in ANA-12 pretreatment group [4.48±0.336 (ANA-12/Blast-HIFN)] is significantly lower than (p=0.003) compared to group which was not given ANA-12 prior to HIFN [7.49±0.487 (Veh/Sham-HIFN)]. N2 amplitude measurements showed a similar trend where improvement in N2 amplitude with HIFN treatment [-9.63±0.580 (Veh/Sham-HIFN) vs –6.54±0.493(Veh/Sham-Veh), p=0.016] was ameliorated with ANA-12 pretreatment [-6.17 ± 0.593 (ANA-12/Sham-HIFN); p= 0.007, w.r.t: Veh/ Sham-HIFN] **Figure 9D**. Taken together, the data showed that ANA-12 administration before HIFN blocked the protective effects of HIFN implicating TrkB dependent neuroprotection by HIFN.

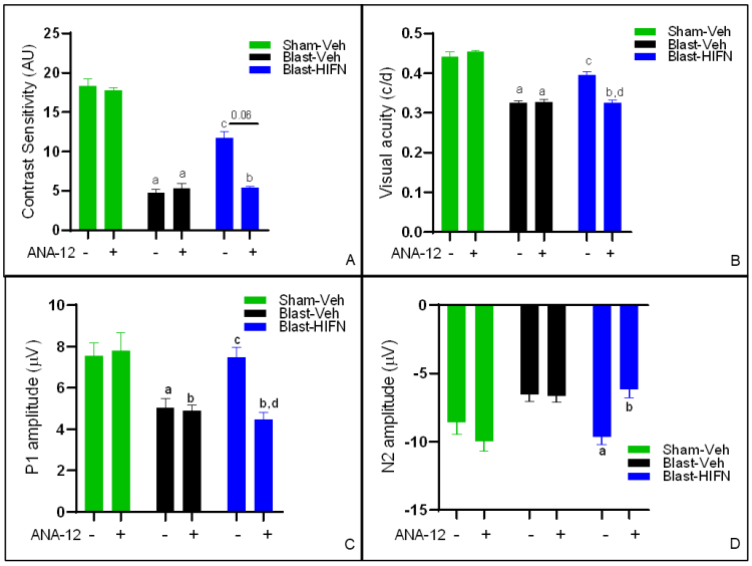

Figure 9. HIFN exerted protection of vision loss is TrkB dependent. ANA-12, a specific TrkB receptor inhibitor, was used to block TrkB activity. Animals were injected with ANA-12 (2.5 h) before the blast. Vehicle or HIFN was then injected within 30 minutes from blast. ANA-12 pretreatment followed by vehicle/HIFN was continued for a week. Contrast sensitivity (A) and visual acuity (B) were measured at 7-weeks post blast and PERG (C and D) recorded at 8-weeks post blast. (A) a=p≤0.0001 vs Veh/Sham-Veh; b=p≤0.001 vs Veh/Sham-Veh; c= p≤0.05 vs Veh/Blast-Veh (B) a=p≤0.0001 vs Veh/Sham-Veh; b=p≤0.001 vs Veh/Sham-Veh; c= p≤0.05 vs Veh/Blast-Veh; d=p≤0.05 vs Veh/Blast-HIFN (C) a=p≤0.05 vs Veh/Sham-Veh; b=p≤0.01 vs Veh/Sham-Veh; c=p≤0.05 vs Veh/Blast-Veh; d=p≤0.01vs Veh/Blast-HIFN (D) a= p≤0.05 vs Veh/Blast-Veh; b=p≤0.01vs Veh/Blast-HIFN; n= 7-9/group

3.4.5. Critical time window for initiating treatment with HIFN

Time for intervention is critical for the effectiveness of any therapeutic drug. To determine the therapeutic treatment window for HIFN, we gave mice an initial treatment at different time intervals after blast, and continued to treat daily for another 6 days. Each group of animals received a 40mg/kg dose of HIFN starting at 0.25, 1, 3, 6 or 24 h post blast. Changes in contrast sensitivity and visual acuity, as well as RGC function (PERG) were recorded at the 7-week and 8-week post blast, respectively. HIFN treatment provided within 3 h of injury significantly reduced vision loss in the animals (**Figure 10**). Beyond the 3h time-window HIFN loses its efficacy in reducing the visual function decline.

Contrast sensitivity was preserved with HIFN treatment even if treatment is delayed up to 3h (49.2±2.90%, p=0.014; **Figure 10A**). However, the best response was found if treatment is provided within 1 h, 60.7±5.46% (p=0.0001) for 0.25h and 57.9±4.61%, (p=0.0001) for the 1 h group compared to 33.6±1.57% for vehicle treated animals. Visual acuity deficit was also best preserved if treatment window does not exceed 3h (**Figure 10B**). Visual acuity was comparable in animals treated at 0.25h (0.394±0.005; p=0.0001), 1h (0.393±0.004; p=0.0001) and 3h (0.381±0.006; p=0.0001) after blast and significantly better than Blast-Veh group (0.340 ±0.005). Beyond the 3h time window the visual acuity deficit could not be prevented with HIFN treatment.

PERG results supported visual function data where again the P1 [p=0.0011; p=0.02 and p=0.002 for 0.25h, 1h and 3h respectively w.r.t Blast-Veh] and N2 [p=0.0044; p=0.06; p=0.002 for 0.25h, 1h and 3h respectively w.r.t

Blast-Veh] amplitudes were significantly higher in animals treated with HIFN within a 3-hour window (**Figure 10 C&D**). Delaying the initial treatment beyond 3h resulted in no significant preservation RGC function.

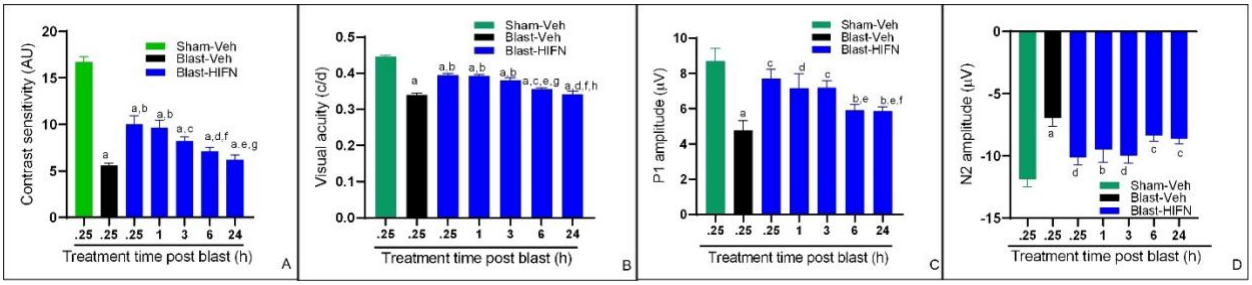

Figure 10. Critical time window for HIFN intervention. Animals were treated with HIFN (40mg/kg) starting at various times relative to blast exposure (treatment time post blast). Treatment was provided as early as 15 minutes (0.25h) after blast and delayed up to 24 h. All mice continued to receive daily treatment for the next 6 days. Contrast sensitivity (A), visual acuity (B), P1 wave amplitude (C) and N2 wave amplitude (D) were recorded. HIFN did not significantly prevent vision loss if the initial reatment was delayed beyond the 3h time window.
(A) a= p≤0.0001 vs Sham-Veh; b=p≤0.0001 vs Blast-Veh; c= p≤0.05 vs Blast-Veh; mg/kg; d= p≤0.05 vs 0.25 h; e= p≤0.001 vs 0.25h; f = p≤ 0.05 vs 1h; g = p≤0.01 vs 1h (B) a= p≤0.0001 vs Sham-Veh; b=p≤0.0001 vs Blast-Veh; c= p≤0.001 vs 0.25h; d= p≤0.0001 vs 0.25h; e= p≤0.001 vs 1h; f = p≤ 0.0001vs 1h; g = p≤0.05 vs 3h; h = p≤0.001 vs 3h; (C) a= p≤0.0001 vs Sham-Veh; b=p≤0.01 vs Sham-Veh; c= p≤0.01 vs Blast-Veh; d= p≤0.05 vs Blast-Veh; e= p≤0.05 vs 0.25h; f = p≤ 0.05 vs 3h; D) a= p≤0.0001 vs Sham-Veh; b=p≤0.05 vs Sham-Veh; c= p≤0.01 vs Sham-Veh; d= p≤0.01 vs Blast-Veh; n= 6-8/group

3.4.6. HIFN protects against traumatic optic neuropathy in both sexes.

The comprehensive study to test the protective effects and efficacy of HIFN was performed on male C57BL/6J mice. To determine if these effects of compounds are not sex-specific, we also induced trauma in female C57 mice and recorded visual function deficit in HIFN treated and non-treated females after one week of treatment. The treatment with HIFN was able to prevent the visual function decline as shown (**Figure 11 A&B**) in both male and female mice. Contrast sensitivity and visual acuity was better in animals treated with HIFN irrespective of sex.

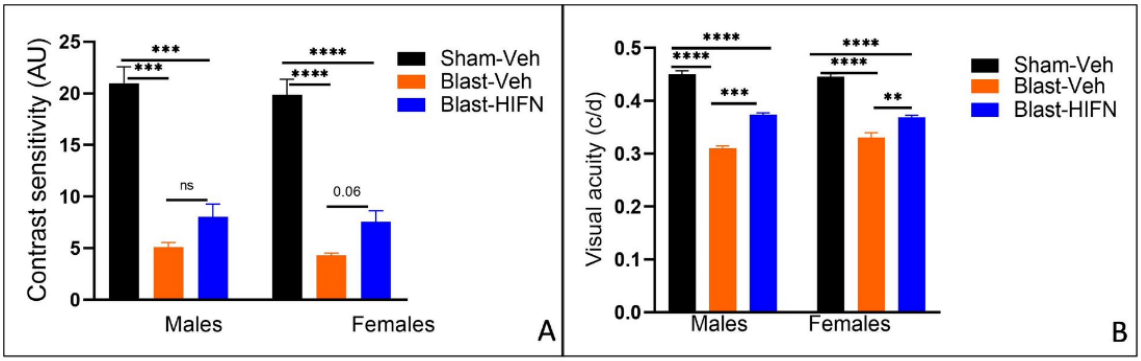

Figure 11. HIFN reduced visual function deficits in both male and female mice. Contrast sensitivity (A) and visual acuity (B) were significantly better in animals treated with HIFN compared to control after one week of blast. **p≤0.01, ***p ≤0.001, ****p≤0.0001

3.4.7. Dose response study for HIFN: Best responses were exhibited at 30mg/kg

In the studies described above, HIFN showed improved visual functions when administered at a dose of 40 mg/kg ip. We performed a dose response series for HIFN to find an optimal dose for neuroprotection (**Figure 12**). HIFN was injected into animals at a dose ranging from 1-100 mg/kg. Contrast sensitivity, visual acuity, and PERG recordings at 7-week post blast showed dose dependent preservation of visual functions. A significant improvement in contrast sensitivity was seen starting from 10mg/kg [34.2± 1.17 (Blast-10mg/kg) vs 24.2± 2.31

(Blast-Veh) p=0.08] and continuing to improve with 30mg/kg (57.9±2.54, p=0.0001 vs Blast-10mg/kg) and 100 mg/kg (50.9± 2.27, p=0.0001 vs Blast-10mg/kg) (**Figure 12A**). Interestingly, contrast sensitivity with 100mg/kg dose showed a marginal but non-significant decline in CS compared to 30mg/kg. Likewise, visual acuity increased significantly from 1mg/kg to 100mg/kg HIFN (p<0.001). HIFN dose of as low as 3mg/kg was effective in visual acuity preservation compared to vehicle (p=0.019). Preservation of visual acuity was observed with a maximally effective dose of 30mg/kg [0.390±0.002, p=0.0001 vs 0.310±0.008 (Blast-Veh)] (**Figure 12B**).

RGC function, as assessed by PERG P1 and N2 amplitudes, also showed a maximal preservation with 30 mg/kg of HIFN (**Figure 12C&D**). Lower doses of HIFN (1, 3 and 10mg/kg) were ineffective in rescuing RGC damage. Animals treated with 1 mg/kg [P1=5.93±0.39; N2=-8.55±0.396], 3 mg/kg [P1=5.70±0.26; N2=-7.39±0.448] and 10mg/kg [P1=5.94±0.30; N2=-7.93±0.456] have unaltered RGC function compared to vehicle treated animals [P1=5.42±0.33; N2=-7.38±0.683]. The only dose that could effectively prevent decline in RGC wave amplitudes is 30mg/kg [P1=8.20±0.34, p=0.013 w.r.t to Blast-Veh; N2=-10.6±0.53, p=0.004 w.r.t Blast-Veh]. The highest dose tested (100mg/kg) had significantly improved N2 amplitude (p=0.04 w.r.t Blast-Veh).

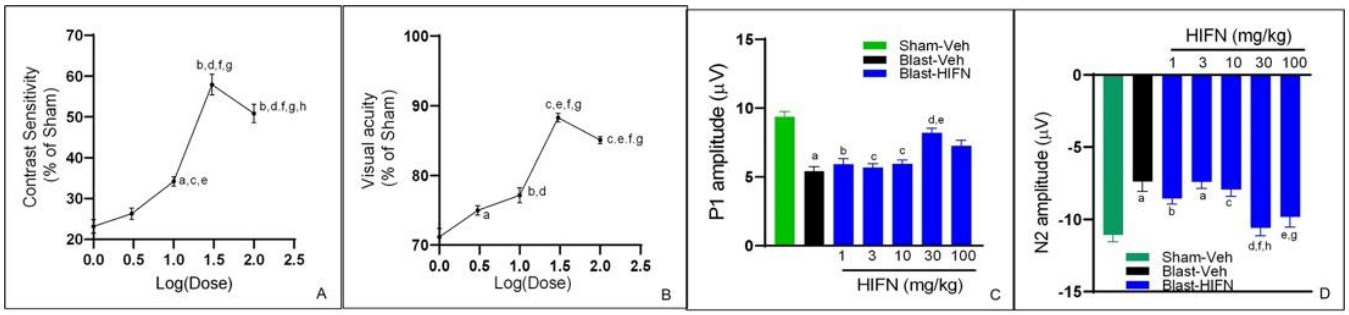

Figure 12. Dose dependent neuroprotection by HIFN. Contrast sensitivity (A) and visual acuity (B) showed a dose dependent improvement at 7-week post blast. Contrast sensitivity started to improve with 10mg/kg dose while visual acuity deficit was reduced even with a low dose of 3mg/kg. RGC cell dysfunction (C and D) was prevented only with 30mg/kg dose.
(A) a= p≤0.01 vs 0mg/kg; b=p≤0.0001vs 0mg/kg; c= p≤0.01 vs 1 mg/kg; d= p≤0.001 vs 1mg/kg; e= p≤0.05 vs 3mg/kg; f= p≤0.0001 vs 3mg/kg; g=p= p≤0.0001 vs 10mg/kg; h= p≤0.05 vs 30mg/kg (B) a= p≤0.05 vs 0mg/kg; b=p≤0.001vs 0mg/kg; c= p≤0.0001 vs 0 mg/kg; d= p≤0.001 vs 1mg/kg; e= p≤0.0001 vs 1mg/kg; f= p≤0.0001 vs 3mg/kg; g= p≤0.0001 vs 10mg/kg (C) a= p≤0.001 vs Sham-Veh; b=p≤0.05 vs Sham-Veh; c= p≤0.01 vs Sham-Veh; mg/kg; d= p≤0.05 vs Blast-Veh; e= p≤0.05 vs 3mg/kg (D) a= p≤0.001 vs Sham-Veh; b=p≤0.05 vs Sham-Veh; c= p≤0.01 vs Sham-Veh; mg/kg; d= p≤0.01 vs Blast-Veh; e= p≤0.05 vs Blast-Veh; f = p≤ 0.01vs3mg/kg; g = p≤0.05 vs 3mg/kg; h = p≤0.05 vs 10mg/kg; n= 6-8/group

3.5. Acute and Chronic Toxicity and Blood Chemistry

3.5.1. Acute Toxicity. We attempted to determine a lethal dose 50 (LD50) for HIFN. To test the acute toxicity of HIFN, both sexes of animals were treated with 300mg/kg of HIFN, a dose 10 times the maximally effective dose in preserving visual function. Mice were monitored for toxicity (piloerection, change in fur color, lethargy, red secretions around eye, hunched back, tremors, weight loss) or mortality for 7 days. No mortality or any signs of toxicity were observed at this dose. We then tested another cohort of animals with a higher dose (600mg/kg). Even at this dose all animals were active, and no visible signs of toxicity were seen. We were unable to test higher doses due to drug solubility issues or determine an LD50. However, we conclude that acute toxicity of HIFN is undetectable.

3.5.2. Chronic Toxicity – Blood Chemistry

Male and female mice were treated with 40 mg/kg of HIFN or vehicle for 40 days. Blood was collected for serum biochemistry analysis and complete blood counts (CBC). No significant differences were observed in serum biochemistry in either males or females (Table 1). No significant changes in CBC parameter were observed in males (Table 2). In females, HIFN treated animals had significantly increased numbers of white blood cells and lymphocytes. Other than these, all other parameters were comparable to vehicle-treated controls.

Table 1. Serum biochemistry of HIFN and vehicle treated male and female mice

Test	Male			Female		
	Vehicle	HIFN	p-value	Vehicle	HIFN	p-value
ALB (g/dL)	2.44±0.24	2.56±0.074	0.80	2.7±0.08	2.55±0.09	0.33
ALP (U/L)	37.6±6.46	39.6±1.32	0.297	70.3±5.49	64.16±2.53	0.332
ALT (U/L)	47.6±8.84	58.8±9.47	0.412	64.33±18.51	61.66±4.93	0.89
AMYL (U/L)	836.8±224.44	668.8±24.72	0.478	624.667±28.09	553.5±42.85	0.08
AST (U/L)	533.2±126.67	473.2±80.59	0.690	467.33±131.09	510±89.60	0.79
BA-SEK (µmol/L)	19.9±9.92	8.82±1.00	0.30	32.45±20.27	22.72±7.83	0.818
BUN (mg/dl)	29.6±3.96	26±3.63	0.53	22.33±1.58	19.5±1.087	0.339
CREAT (mg/dl)	0.272±0.05	0.424±0.03	0.051	0.35±0.04	0.43±0.04	0.206
DBILI (mg/dl)	0.44±0.16	0.44±0.07	0.99	0.36±0.08	0.35±0.06	0.99
LDH (U/L)	1414.8±317.82	1258.8±198.41	0.68	1037.33±294.24	1215.83±193.63	0.62
TBILI (mg/dl)	0.556±0.116	0.476±0.05	0.54	0.413±0.06	0.49±0.07	0.461

N= 6 animals/group

Table 2: CBC profile of HIFN and vehicle treated male and female mice

Blood Test	Male			Female		
	Vehicle	HIFN	p-value	Vehicle	HIFN	p-value
White blood cells (per liter)	$1.52*10^9$	$2.46*10^9$	0.081	$1.11*10^9$	$2.03*10^9$	0.004
Lymphocytes (per liter)	$1.36*10^9$	$2.25*10^9$	0.082	$1.03*10^9$	$1.92*10^9$	0.003
Monocytes (per liter)	$0.053*10^9$	$0.056*10^9$	0.90	$0.03*10^9$	$0.04*10^9$	0.61
Neutrophils (per liter)	$0.103*10^9$	$0.151*10^9$	0.53	$0.05*10^9$	$0.07*10^9$	0.56
Lymphocyte (%)	89.72	91.85	0.48	91.87	94.85	0.10
Monocyte (%)	3.52	2.47	0.57	2.88	1.93	0.25
Neutrophils (%)	6.78	5.68	0.73	5.25	3.20	0.24
Red blood cells (per liter)	$8.28*10^{12}$	$8.25*10^{12}$	0.99	$8.88*10^{12}$	$8.05*10^{12}$	0.14
Hemoglobin (g/liter)	10.73	10.68	0.90	11.95	10.55	0.09
Hematocrit (%)	34.87	35.31	0.72	37.56	34.12	0.17
Mean corpuscular volume (fl)	42.17	42.83	0.31	42.00	42.33	0.87
Mean corpuscular Hb (pg)	12.93	12.93	0.99	13.45	13.12	0.21
Mean corpuscular Hb conc (g/liter)	30.75	30.20	0.053	32.00	30.92	0.06
RDWc (%)	19.55	19.98	0.28	20.10	20.45	0.26
RDWs (fl)	30.72	32.17	0.09	31.92	32.55	0.47
Platelet (per liter)	$170.33*10^9$	$276.5*10^9$	0.30	$340.00*10^9$	$298.33*10^9$	0.69
Mean platelet volume (fl)	8.08	6.70	0.73	6.30	7.52	0.67
Plateletcrit (%)	0.12	0.18	0.28	0.22	0.19	0.32
PDWc (%)	25.80	27.33	0.96	28.22	25.10	0.20
PDWs (fl)	8.83	8.17	0.62	8.28	8.07	0.48

N=6 animals/group

3.5.3. Chronic toxicity – Histopathology

Male and female mice were treated with 40 mg/kg of HIFN or vehicle for 40 days. Brain, eye, liver, kidney, spleen, testes/ovary, heart tissue was harvested, and sections were analyzed for histopathology. Representative sections are shown in **Figure 13.** The specimens were evaluated by Dr. Hans Grossniklaus, MD, MBA, a board certified pathologist. No abnormal changes due to HIFN toxicity were reported.

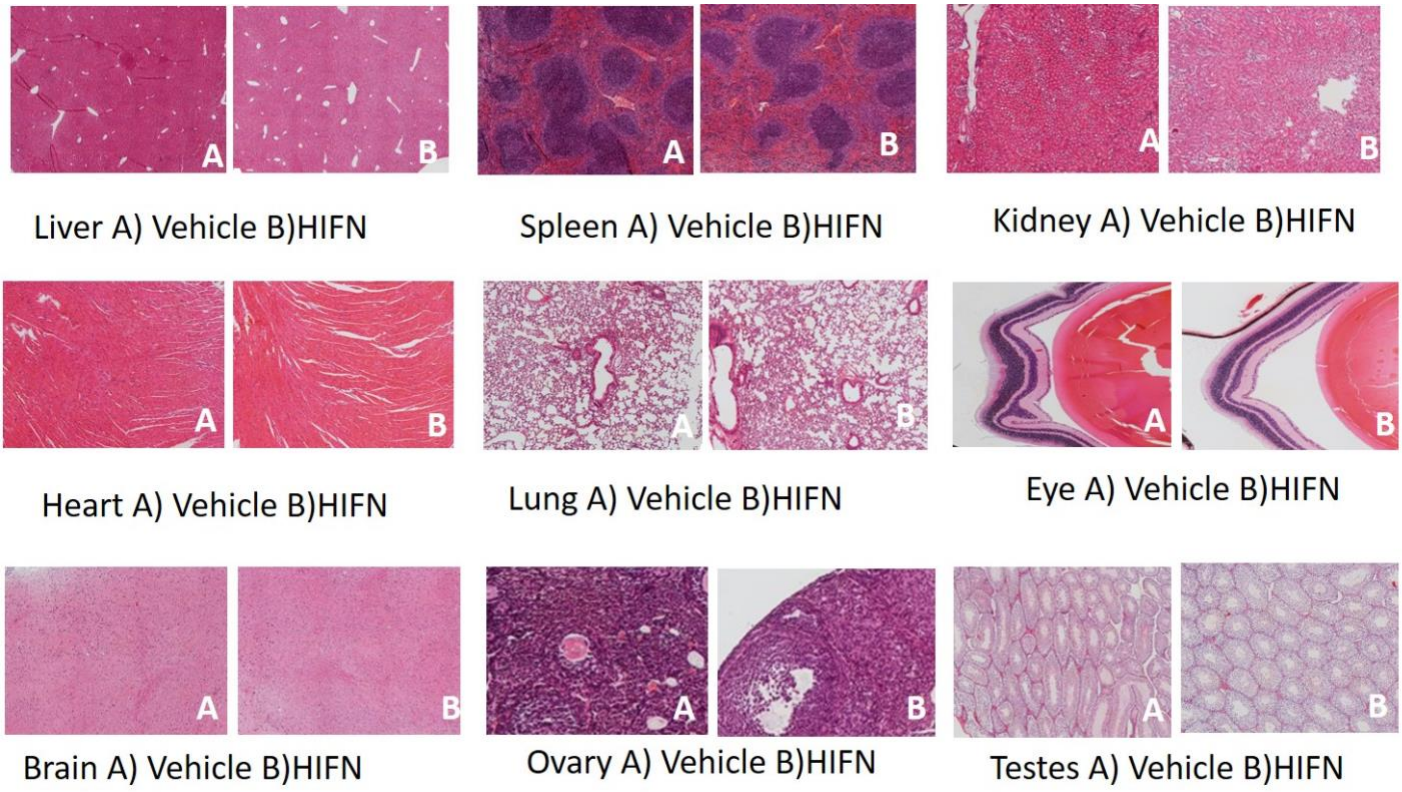

Figure 13. Representative images of hematoxylin/eosin-stained tissue sewction from mice treated with HIFN or vehicle for 40 days.

3.6. Other achievements: During the COVID-19 pandemic lockdown in spring 2020, Dr. Walker initiated a computational modeling project consistent with the project goals, probing possible binding sites for *N*-acetylserotonin with the active domain of TrkB (an endogenous but short-lived activator), and searches for similarities in binding with each enantiomer of HIOC. The computational work was based on crystal structures of TrkB, with the best results arising from structure 1WWB (Protein Data Bank), of a portion of the immunoglobulin domain-2 (or TrkB domain 5), observing similar binding affinities between *N*-acetylserotonin (NAS) and each enantiomer of HIOC. This work examined binding with grid boxes from residues S294-N365, and specific residues H335 and H343.

ligands	1WWB: S294-N365	1WWB: H335 and H343
NAS	-7.7 kcal mol^{-1}	-2.9 kcal mol^{-1}
(*R*)-HIOC	-8.0 kcal mol^{-1}	-2.4 kcal mol^{-1}
(*S*)-HIOC	-7.1 kcal mol^{-1}	-4.1 kcal mol^{-1}

Table 3. Calculated binding affinity comparison of *N*-acetylserotonin (NAS) with each enantiomer of HIOC

3.7. Stated goals not met:

Almost all of the proposed synthetic analogs were successfully prepared. Two of the analogs envisioned in series **B** were difficult or impossible to prepare, due to facile decarboxylation of carboxylic acid precursors. We also attempted to synthesize an enantiomerically enriched *C*-methyl analog of HIOC, as well as ring-size analogs of the six-membered lactam of HIOC. However, the literature procedures for precursor compounds supporting these two minor aims were not reproducible. While we made some progress toward solving these problems, the work was not completed before the grant had expired. These analogs were similar to some of our less active analogs, so the urgency to prepare the few remaining analogs proposed in series **B** diminished as we learned more about the excellent biological qualities of our best candidate compound, HIFN.

Pharmacokinetic analysis: blood samples were collected and frozen just before the grant ended. However, both Dr. Modgil and our technician left to take new positions before the HPLC analysis of the samples was completed. A new technician will join the Iuvone lab in early spring, and we will analyze the samples.

- **What opportunities for training and professional development has the project provided?**

Co-PI Prof. McDonald and Dr. Walker mentored two undergraduate students, Taylor Dover and Tiffany Hung, who assisted with synthetic chemistry portions of this project. Both students defended senior honors theses which in part described their synthetic chemistry research. Taylor Dover is currently a chemistry graduate student at Yale University, and Tiffany Hung is currently a chemistry graduate student at California Institute of Technology.

- **How were the results disseminated to communities of interest?**

Nothing to report

- **What do you plan to do during the next reporting period to accomplish the goals?**

Nothing to report, as this is the final report.

4. IMPACT:

- **What was the impact on the development of the principal discipline(s) of the project?**

Although inhibitors of TrkB phosphorylation have been developed as medicinal agents, drugs that *activate* the TrkB receptor have not been reported. Our recent findings with HIFN potentially provide the first rationally designed therapeutic agents to promote healing retinas damaged from blast or blunt force trauma.

- **What was the impact on other disciplines?**

The structure of HIFN and our synthetic route appears to be suitable for near-term future research into an HIFN ^{18}F-radiotracer for positron emission tomography (PET) imaging.

- **What was the impact on technology transfer?**

Our office of technology transfer has received preliminary licencing inquiries from two biotechnology companies.

- **What was the impact on society beyond science and technology?**

Ongoing military conflicts in other parts of the world, and the unfortunate prospect of near-term future conflicts, mean that there remains an urgent, unmet need for more effectively treating eye injuries incurred by military combatants and non-combatant civilians.

5. CHANGES/PROBLEMS:

- **Changes in approach and reasons for change**

The COVID-19 pandemic adversely affected research progress beginning in March 2020. As the laboratories were closed for several months, we initiated a computational chemistry project toward these research aims that continued parallel with laboratory research after the laboratories reopened in June 2020.

- **Actual or anticipated problems or delays and actions or plans to resolve them**

The biggest problem was the sudden shutdown of virtually all Emory University laboratories from mid-March 2020 through the end of May 2020, due to the COVID-19 pandemic. Although we resumed in-person laboratory work in June 2020, the ongoing pandemic had disruptive effects on productivity for the remainder of the grant period. We were also hampered by a year-long hiring freeze due to the pandemic, which prevented us from hiring an additional postdoctoral associate for the biological assessment of the HIOC analogs, although we had sufficient funding at that time. Ultimately we requested and received a no-cost extension year, which allowed for the research to continue with the existing personnel.

- **Changes that had a significant impact on expenditures**

Dr. Christopher Walker's salary and benefits were supported by the NIH Vision Training Grant for about three years of the grant period. We rebudgeted the funding to support the one year no cost extension.

Significant changes in use or care of human subjects, vertebrate animals, biohazards, and/or select agents

- **Significant changes in use or care of human subjects**

  Nothing to report

- **Significant changes in use or care of vertebrate animals.**

  Nothing to report

- **Significant changes in use of biohazards and/or select agents**

  Nothing to report

6. PRODUCTS:

- **Publications, conference papers, and presentations**
  Report only the major publication(s) resulting from the work under this award.

  - **Journal publications.**

Susov Dhakal, Li He, Polina Lyuboslavsky, Currin Sidhu, Micah A. Chrenek, Jana T. Sellers, Jeffrey H. Boatright, Eldon E. Geisert, Noah A. Setterholm, Frank E. McDonald, P. Michael Iuvone. A TrkB Receptor Activator for the Treatment of Ocular Blast-Induced Vision Loss. *J. Neurotrauma*, 2021;38:2896-2906. doi: 10.1089/neu.2020.7392. PMID: 34353120.
Acknowledgement of federal support – yes. A copy of paper is attached in the Appendix.

(Four additional manuscripts are in preparation)

- **Books or other non-periodical, one-time publications.**

  Nothing to report

- **Other publications, conference papers, and presentations.**

Modgil S, Walker CL, McDonald FE, Iuvone PM. 2-Fluoro[N-(2-(5-hydroxy-1H-indol-3-yl) ethyl)nicotimamide (HIFN) protects against vision loss from closed-globe ocular trauma by activating tropomyosin-related kinase B (TrkB). *Invest Ophthalmol Vis Sci* 2022;63:1485 (ARVO meeting abstract). *Acknowledgement of federal support – yes.*

Modgil S, Walker CL, McDonald FE, Iuvone PM. A novel tropmyosin-related kinase-B (TrkB) receptor agonist prevents vision loss after blast overpressure injury. *Journal of Neurotrauma* 2022;39(11-12). (The 39th Annual Symposium of the National Neurotrauma Society) *Acknowledgement of federal support – yes.*

Modgil S, Walker C, McDonald F, Iuvone M. A novel small molecule tropomyosin-related kinase-B (TrkB) receptor activator: HIFN (2-fluoro-N-(2-(5-hydroxy-1H-indol-3-yl)ethyl)nicotinamide). *J Neurochem* 2022;162 Issue S1. (ISN-APSN 2022 Meeting) *Acknowledgement of federal support – yes.*

- **Website(s) or other Internet site(s)**
  Nothing to report

- **Technologies or techniques**
  Nothing to report

- **Inventions, patent applications, and/or licenses**

The provisional U.S. patent application submitted by Emory University in 2019 "*N*-Acetylserotonin Derivatives as TrkB Activators and Uses Thereof." has been re-filed as an International PCT Application as of October 2022, including as co-inventors Dr. Paul Michael Iuvone, Dr. Frank Edward McDonald, and Dr. Christopher Lee Walker. Serial number PCT/US2021/029908

- **Other Products**
  Nothing to report.

7. PARTICIPANTS & OTHER COLLABORATING ORGANIZATIONS

- **What individuals have worked on the project?**

Name:	Paul Michael Iuvone
Project Role:	Principal Investigator
Researcher Identifier (e.g. ORCID ID):	miuvone
Nearest person month worked:	14
Contribution to Project:	Dr. Iuvone organized and coordinated research team activities, regulatory protocols (IACUC/ACURO), and planning
Funding Support:	this award

Name:	Frank Edward McDonald
Project Role:	Co-PI
Researcher Identifier (e.g. ORCID ID):	FRANK_MCDONALD
Nearest person month worked:	12
Contribution to Project:	Dr. McDonald supervised all synthetic work, the computational research, and assisting with ongoing manuscript preparations.
Funding Support:	this award

Name:	Christopher L. Walker
Project Role:	Postdoctoral associate
Researcher Identifier (e.g. ORCID ID):	CWALKE
Nearest person month worked:	47
Contribution to Project:	Dr. Walker conducted the synthetic and computational modeling work in this project.
Funding Support:	this award; NIH Vision Training Grant

Name:	Shweta Modgil
Project Role:	Postdoctoral associate
Researcher Identifier (e.g. ORCID ID):	SMODGIL
Nearest person month worked:	30
Contribution to Project:	Dr. Modgil conducted most of the in vitro and in vivo characterization of the analogs.
Funding Support:	this award

Name:	Dwipayan Bhattacharya
Project Role:	Postdoctoral associate
Researcher Identifier (e.g. ORCID ID):	DBHAT24
Nearest person month worked:	12
Contribution to Project:	Dr. Bhattacharya conducted some initial in vitro assay development to assess TrkB activation.
Funding Support:	this award

Name:	Hans E. Grossniklaus
Project Role:	Co-investigator
Researcher Identifier (e.g. ORCID ID):	HANS_E _GROSSNIKLAUS
Nearest person month worked:	1
Contribution to Project:	Dr. Grossniklaus evaluated the tissue histopathology in the toxicology study.
Funding Support:	this award

Name:	Taylor Dover
Project Role:	Undergraduate student researcher
Researcher Identifier (e.g. ORCID ID):	TDOVER
Nearest person month worked:	3

Contribution to Project:	Mr. Dover assisted Dr. Walker with chemical synthesis.
Funding Support:	none

Name:	Tiffany Hung
Project Role:	Undergraduate student researcher
Researcher Identifier (e.g. ORCID ID):	TIFFHUNG
Nearest person month worked:	5
Contribution to Project:	Ms. Hung assisted Dr. Walker with chemical synthesis, and also drafted a review article relevant to this research area.
Funding Support:	this award

- **Has there been a change in the active other support of the PD/PI(s) or senior/key personnel since the last reporting period?**

Co-PI Frank E. McDonald received a seed grant for unrelated medicinal chemistry research:
Title: "Repurposing and modifying known drugs for chemoresistant prostate cancer"
Source: Biological Discovery through Chemical Innovation (BDCI) initiative at Emory University.
Dates: April 1, 2022 - October 31, 2022
Amount:

Co-PI Frank E. McDonald closed / completed a grant for unrelated synthetic methods research:
Title: "Overcoming Steric Challenges in Glycosylation"
Source: National Institutes of Health, R21GM127971
Dates: April 1, 2018 - March 31, 2022
Amount:

- **What other organizations were involved as partners?**

  Nothing to report

8. SPECIAL REPORTING REQUIREMENTS

- **QUAD CHARTS:** *see attachments*

9. APPENDICES:

APPENDIX

1. Catalog of analogs synthesized.

2. Susov Dhakal, Li He, Polina Lyuboslavsky, Currin Sidhu, Micah A. Chrenek, Jana T. Sellers, Jeffrey H. Boatright, Eldon E. Geisert, Noah A. Setterholm, Frank E. McDonald, P. Michael Iuvone. A TrkB Receptor Activator for the Treatment of Ocular Blast-Induced Vision Loss. *J. Neurotrauma*, 2021;38:2896-2906.

3. Modgil S, Walker CL, McDonald FE, Iuvone PM. 2-Fluoro[N-(2-(5-hydroxy-1H-indol-3-yl) ethyl)nicotimamide (HIFN) protects against vision loss from closed-globe ocular trauma by activating tropomyosin-related kinase B (TrkB). *Invest Ophthalmol Vis Sci* 2022;63:1485 (ARVO meeting abstract).

4. Modgil S, Walker CL, McDonald FE, Iuvone PM. A novel tropmyosin-related kinase-B (TrkB) receptor agonist prevents vision loss after blast overpressure injury. *Journal of Neurotrauma* 2022;39(11-12). (The 39th Annual Symposium of the National Neurotrauma Society abstract).

5. Modgil S, Walker C, McDonald F, Iuvone M. A novel small molecule tropomyosin-related kinase-B (TrkB) receptor activator: HIFN (2-fluoro-N-(2-(5-hydroxy-1H-indol-3-yl)ethyl)nicotinamide). *J Neurochem* 2022;162 Issue S1. (ISN-APSN 2022 Meeting abstract).

Series A Compounds

Design Objective: the specific aim of series A is to systematically replace hydrogen bond donors with methyl groups to increase lipophilicity, decrease polar surface area, and elucidate essential elements of pharmacophore regarding hydrogen bonding. In some cases, hydrogen bond donors were replaced with hydrogen or with fluorine.

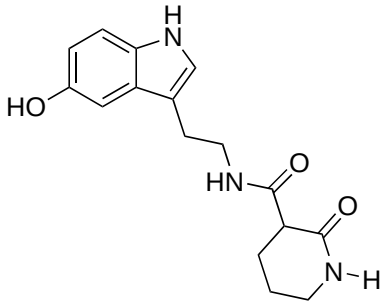

HIOC

N-(2-(5-hydroxy-1H-indol-3-yl)ethyl)-2-oxopiperidine-3-carboxamide (HIOC)

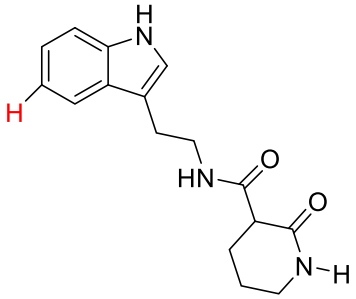

N-(2-(1H-indol-3-yl)ethyl)-2-oxopiperidine-3-carboxamide (**145**)

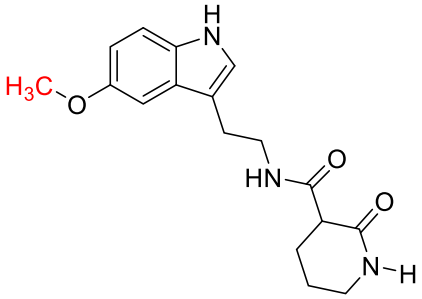

N-(2-(5-methoxy-1H-indol-3-yl)ethyl)-2-oxopiperidine-3-carboxamide (**149**)

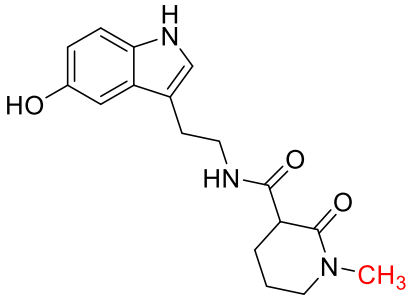

N-(2-(5-hydroxy-1H-indol-3-yl)ethyl)-1-methyl-2-oxopiperidine-3-carboxamide (**151**)

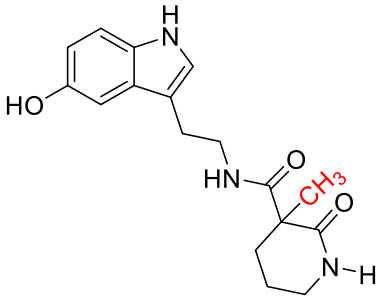

N-(2-(5-hydroxy-1H-indol-3-yl)ethyl)-3-methyl-2-oxopiperidine-3-carboxamide (**170**)

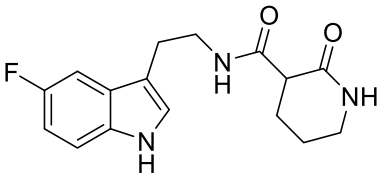

N-(2-(5-fluoro-1H-indol-3-yl)ethyl)-2-oxopiperidine-3-carboxamide (**177**)

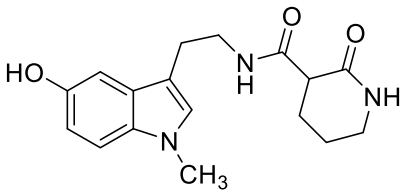

N-(2-(5-hydroxy-1-methyl-1H-indol-3-yl)ethyl)-2-oxopiperidine-3-carboxamide (**201**)

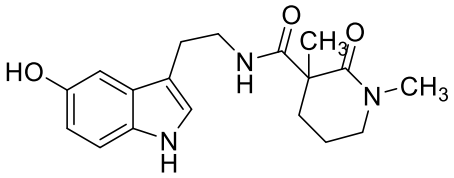

N-(2-(5-hydroxy-1H-indol-3-yl)ethyl)-1,3-dimethyl-2-oxopiperidine-3-carboxamide (**35**)

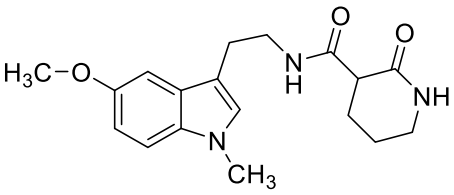

N-(2-(5-methoxy-1-methyl-1H-indol-3-yl)ethyl)-2-oxopiperidine-3-carboxamide(**196**)

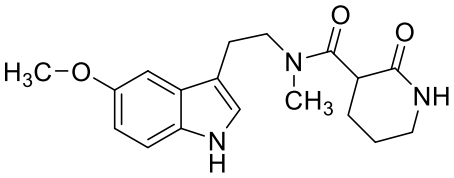

N-(2-(5-methoxy-1H-indol-3-yl)ethyl)-N-methyl-2-oxopiperidine-3-carboxamide (**217 or 203**)

Series B Compounds

Design Objective: This series was designed to systematically alter hydrogen bond accepting beta-dicarbonyl function, testing if these changes increase or decrease lipophilicity were restraining six-membered ring of N-acyl substituent.

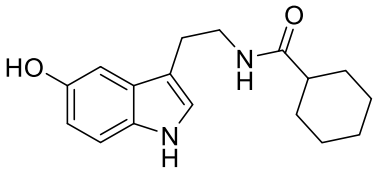

N-(2-(5-hydroxy-1H-indol-3-yl)ethyl)cyclohexanecarboxamide (**187**)

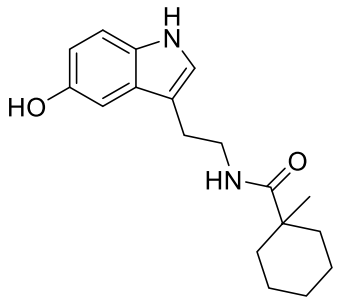

N-(2-(5-hydroxy-1H-indol-3-yl)ethyl)-1-methylcyclohexane-1-carboxamide (**189**)

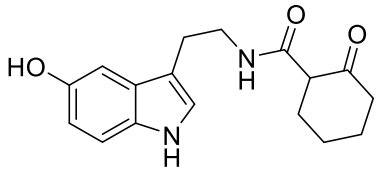

N-(2-(5-hydroxy-1H-indol-3-yl)ethyl)-2-oxocyclohexane-1-carboxamide **(211)**

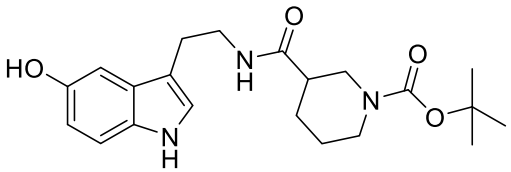

(+/-) tert-butyl 3-((2-(5-hydroxy-1H-indol-3-yl)ethyl)carbamoyl)piperidine-1-carboxylate (**229**)

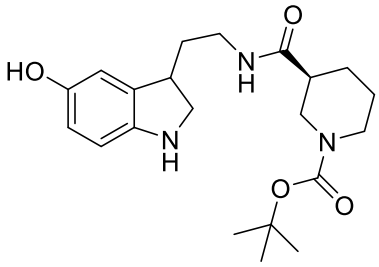

Tert-butyl (3S)-3-((2-(5-hydroxyindolin-3-yl)ethyl)carbamoyl)piperidine-1-carboxylate (**265**)

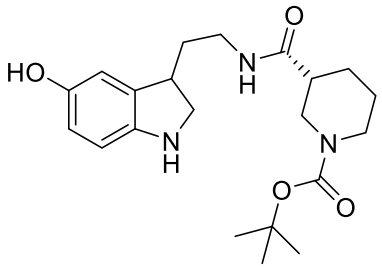

Tert-butyl (3R)-3-((2-(5-hydroxyindolin-3-yl)ethyl)carbamoyl)piperidine-1-carboxylate (pg **269**)

Series C Compounds

Design Objective: Incorporation of aromatic and heteroaromatic rings which are observed in common drug compounds. This addition also eliminates the chiral center observed in HIOC. Incorporation of pyridine rings test hydrogen bond accepting properties of pyridine nitrogen.

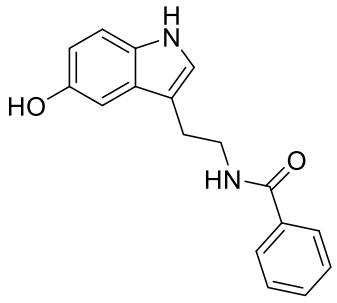

N-(2-(5-hydroxy-1H-indol-32-yl)ethyl)benzamide (**83**)

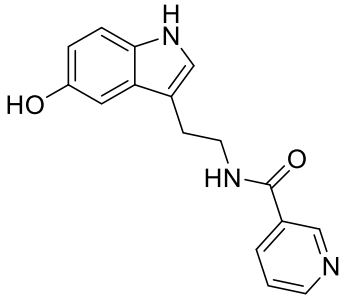

N-(2-(5-hydroxy-1H-indol-3-yl)ethyl)nicotinamide (**85**)

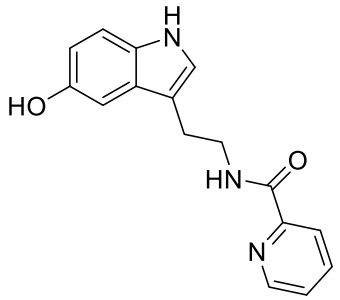

N-(2-(5-hydroxy-1H-indol-3yl)ethyl)picolinamide (**105**)

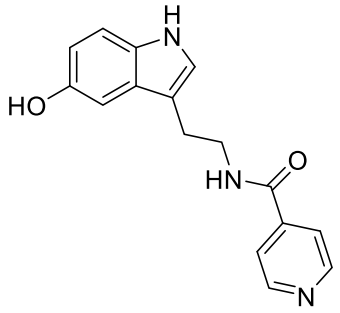

N-(2-(5-hydroxy-1H-indol-3-yl)ethyl)isonicotinamide (**107**)

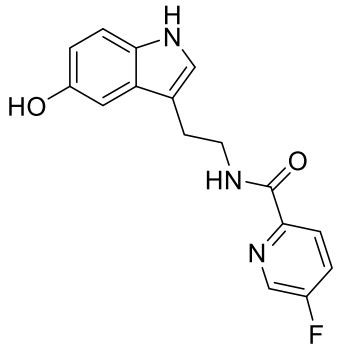

5-fluoro-*N*-(2-(5-hydroxy-1H-indol-3yl)ethyl)picolinamide (**112**)

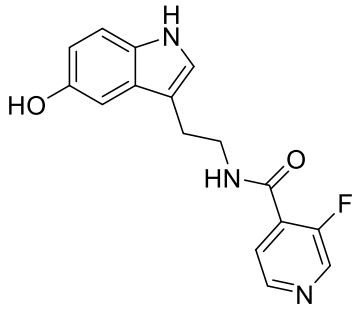

3-fluoro-*N*-(2-(5-hydroxy-1H-indol-3-yl)ethyl)isonicotinamide (**114**)

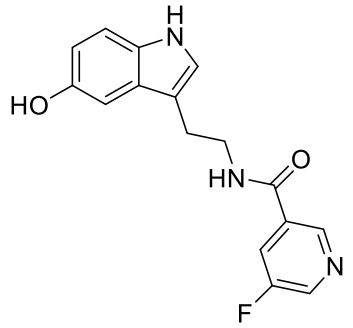

5-Fluoro-*N*-(2-(5-hydroxy-1H-indol-3-yl)ethyl)nicotinamide (**127**)

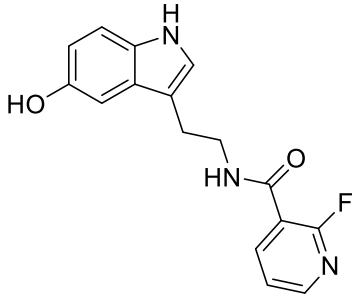

2-fluoro-N-(2-(5-hydroxy-1H-indol-3yl)ethyl)nicotinamide (**147-HIFN**)

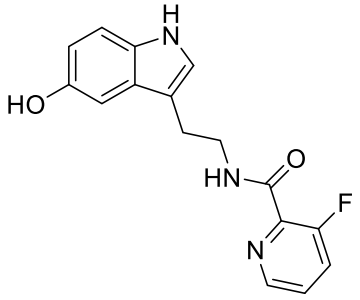

3-fluoro-N-(2-(5-hydroxy-1H-indol-3-yl)ethyl)picolinamide (**118**)

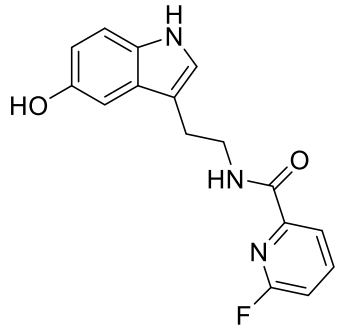

6-fluoro-N-(2-(5-hydroxy-1H-indol-3-yl)ethyl)picolinamide (**172**)

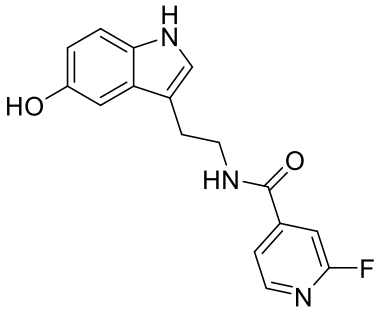

2-fluoro-N-(2-(5-hydroxy-1H-indol-3-yl)ethyl)isonicotinamide(**168)**

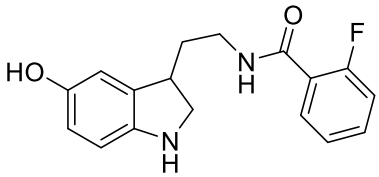

2-Fluoro-N-(2-(5-hydroxy-1H-indol-3-yl)ethyl) benzamide (pg **263**)

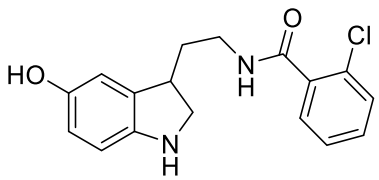

2-chloro-N-(2-(5-hydroxyindolin-3-yl)ethyl)benzamide **(NB2-11)**

Journal of Neurotrauma
38:2896–2906 (October 15, 2021)

DOI: 10.1089/neu.2020.7392

Journal of Neurotrauma

ORIGINAL ARTICLE TRANSLATIONAL THERAPEUTICS

A Tropomycin-Related Kinase B Receptor Activator for the Management of Ocular Blast-Induced Vision Loss

Susov Dhakal,[1,†] Li He,[1] Polina Lyuboslavsky,[1,‡] Curran Sidhu,[1] Micah A. Chrenek,[1] Jana T. Sellers,[1] Jeffrey H. Boatright,[1] Eldon E. Geisert,[1] Noah A. Setterholm,[2,††] Frank E. McDonald,[2] and P. Michael Iuvone[1,3,*]

Abstract

Pressure waves from explosions or other traumatic events can damage the neurons of the eye and visual centers of the brain, leading to functional loss of vision. There are currently few treatments for such injuries that can be deployed rapidly to mitigate damage. Brain-derived neurotrophic factor (BDNF) and activation of its receptor tropomycin-related kinase B (TrkB) have neuroprotective effects in a number of degeneration models. Small molecule activators of TrkB, such as N-[2-(5-hydroxy-1H-indol-3-yl)ethyl]-2-oxopiperidine-3-carboxamide (HIOC), cross the blood–brain and blood-retina barriers after systemic administration. We characterize the effects of blast-induced ocular trauma on retinal and visual function. We show that systemic administration of HIOC, a potent small molecule activator of the BDNF/TrkB receptor, preserves visual function in mice exposed to ocular blast injury. The HIOC treatment for one week preserves visual function for at least four months. The HIOC treatment effectively protected vision when the initial dose was administered up to 3 h after blast, but not if the initial treatment was delayed for 24 h. We provide evidence that the therapeutic effect of HIOC is mediated by activation of BDNF/TrkB receptors. The results indicate that HIOC may be useful for managing ocular blast injury and other forms of traumatic optic neuropathy.

Keywords: axon injury; BDNF/TrkB receptor; HIOC; neuroprotection; ocular blast injury; traumatic optic neuropathy

Introduction

Vision loss caused by traumatic ocular blast injury, sports injury, automobile accidents, or other blunt force trauma to the eye is a serious public health issue, affecting military personnel and the general public. Traumatic blast injury from improvised explosive devices was the most common cause of craniomaxillofacial injuries during operations Enduring Freedom and Iraqi Freedom,[1] with a high incidence of ocular trauma.[2]

Traumatic blast injury frequently results in vision loss because of ocular damage or insult to the optic nerve and central visual pathways.[3] Blast overpressure is sufficient to induce ocular damage in the absence of any shrapnel, resulting in closed-globe injury and loss of visual function.[4] In cases of traumatic blast-induced ocular injury, the retina may be damaged directly by pressure waves from the explosion[3] or by several other factors, such as shear from percussive forces, penetrating injury, or retrobulbar hemorrhage.[5]

Secondary neuronal loss from factors released from dying neurons may also contribute to vision loss because of death of nearby cells.[6] In addition, traumatic brain injury (TBI) is often associated with visual dysfunction because of damage to central visual pathways.[3] Such damage is not reversible with current therapies.[7,8] To slow or prevent trauma-induced neuronal degeneration in the retina and central visual pathways, a therapy is needed that can be deployed rapidly on the battlefield, in a field hospital, or in the emergency department.

Attempts to simulate battlefield conditions that induce blast injuries in laboratory settings using different animal models have been reported. Pressure waves as low

Departments of [1]Ophthalmology, [2]Chemistry, [3]Pharmacology and Chemical Biology, Emory University, Atlanta, Georgia, USA.
Current affiliations: [†]Department of Physiology, Monash University, Melbourne, Australia; [‡]Department of Neurology, University of Texas at Austin, Austin, Texas, USA; [††]School of Pharmacy and Pharmaceutical Sciences, University of California Irvine, Irvine, California, USA.

*Address correspondence to: *P. Michael Iuvone, PhD, Department of Ophthalmology, Emory University School of Medicine, 1365 Clifton Rd NE, Atlanta, GA 30322, USA*
E-mail: miuvone@emory.edu

as 26 psi cause closed-globe injuries in mice resulting in retinal detachment, pyknotic nuclei in the inner nuclear layer (INL) and outer nuclear layer (ONL), delayed neuronal cell death, gliosis, and diminished visual function.[9] Reduced ganglion cell responses and significant decrease in retinal nerve fiber layer (NFL) thickness three months after blast injury have also been reported in mice.[10]

Similarly, a primary blast wave of 20 psi directed to the eye of adult Sprague-Dawley rats reduced a- and b-wave amplitude of the electroretinogram (ERG) and induced histopathology in the eye and optic tract.[11] Pathological changes in the retina, indicated by increase in expression of inflammatory cytokines, edema, and apoptosis, were observed in rats after primary blast injury to the eye.[12] In Dutch Belted rabbits, blast overpressure caused significant changes in corneal and retinal thickness along with changes in intraocular pressure (IOP).[13] Overall, primary blast overpressure results in damage to the retina and central visual centers, ultimately leading to neurodegeneration.[11]

Brain-derived neurotrophic factor (BDNF) has neuroprotective actions in the adult brain.[14–16] It also has protective effects in the retina, decreasing ganglion cell loss from optic nerve damage[17,18] and photoreceptor loss in bright light-induced retinal degeneration.[19,20] The BDNF, however, must be injected directly into the eye and brain to be effective, because it does not cross the blood–brain barrier (BBB). Protection from optic nerve damage is improved when BDNF is injected into both eye and visual cortex than into the eye alone.[18] Thus, it is impractical to administer BDNF to manage blast-induced eye or brain injury on the battlefield or in emergency vehicles. There are currently few treatments for such injuries that can be deployed rapidly to mitigate such damage.

Tropomycin-related kinase B (TrkB) is the cognate receptor for BDNF.[21–23] The BDNF and small molecule activators of its receptor, N-[2-(5-hydroxy-1H-indol-3-yl)ethyl]-2-oxopiperidine-3-carboxamide (HIOC) and N-acetylserotonin, can protect neurons from apoptosis or promote neurogenesis under different circumstances.[24–26] Unlike BDNF, HIOC crosses the blood–brain and blood-retina barriers after IP injection and protects photoreceptors from light-induced retinal degeneration (LIRD).[25]

The principal mechanism of HIOC action involves a TrkB signaling cascade.[25] As evidence of neuroprotection and TrkB signaling activation, increased phosphorylation of TrkB and Akt were detected in HIOC treated cells and tissues, along with a decrease of neurotoxin-induced caspase-3 activation.[25] Here, we have tested the hypothesis that TrkB receptor activation by HIOC mitigates the loss of visual function in mice exposed to blast overpressure.

Methods

Animals

Mice were maintained in a 12-h light-12-h dark cycle with food and water *ad libitum*. Wild-type C57BL/6J and transgenic Thy1:CFP mice (B6.Cg-Tg(Thy1-CFP)23Jrs/J), expressing cyan fluorescent protein (CFP) in retinal ganglion cells (RGCs) under the Thy1 promoter,[27] were bred in our animal facilities from stock obtained from Jackson Laboratories (Bar Harbor, Maine). Thy1:CFP mice were bred as heterozygotes, and offspring were genotyped by polymerase chain reaction. Thy1:CFP mice were used in experiments where retinal ganglion cells were counted.

All experiments using animals were conducted in accordance with the National Institutes of Health Guide for the Care and Use of Laboratory Animals and under approval of Emory University's Institutional Animal Care and Use Committee. Ketamine/xylazine (87 mg/kg/13 mg/kg) solution was administered IP to anesthetize the mice during experimental procedures, where indicated. Mice were euthanized by overdose of ketamine/xylazine or by asphyxiation with carbon dioxide.

Blast injury procedure

Ocular blast injury was induced as described,[28,29] using an air gun. The mouse eye was positioned behind a 5 mm hole in a clear polyvinyl chloride pipe (3 mm thickness), and the head was supported with padding. The output pressure of the air gun was calibrated to approximately 48 psi using a Honeywell Sensotec sensor Model STJE (0–100 psi) with the probe inserted into the mouse holding pipe directly against the hole, which was positioned directly against the barrel opening of the air gun. The pressure 6 mm from the barrel opening, the approximate position of the mouse eye during the blast procedure,[29] was 20 psi.

Blast was delivered to the right eye of anesthetized mice. At the calibrated output pressure of $\sim$48 psi, there were no instances of ocular rupture. After the blast procedure, the mice were kept on a heating pad until recovered from anesthesia. Mice received an oral analgesic (acetaminophen; 32 mg/mL) before blast exposure and for the next two days. Mice were returned to their cages after they were awake. Sham-treated mice were treated identically, but not exposed to the blast.

HIOC preparation

The HIOC was synthesized as described previously[30] and stored at -20°C under argon. Stock solutions were prepared in dimethylsulfoxide (DMSO) and diluted with sterile H_2O; the final DMSO concentration was 10%. The HIOC and vehicle control solutions were administered by IP injection.

Optomotor response (OMR) testing

Contrast and spatial frequency thresholds were determined as measures of contrast sensitivity and visual acuity (OptoMotry: CerebralMechanics. Inc., Lethbridge, Alberta. Canada).[31,32] Briefly, the mouse was placed on a central elevated platform in the OptoMotry chamber surrounded by four monitors that project a virtual rotating cylinder with sinusoidal gratings of vertical light and dark bars. An infrared camera located on the top of the chamber tracks the behavior of the mouse, which reflexively follows the moving gratings by turning its head.

We examined contrast thresholds at multiple spatial frequencies in sham and blast mice (Fig. 1); in most experiments, they were measured at a spatial frequency of 0.064 cycles/degree (c/d), the peak of contrast sensitivity,[32] and the spatial frequency where blast had its largest effect (Fig. 1). Contrast sensitivity data are expressed as the inverse of the contrast thresholds. Contrast sensitivity is regulated in a circadian manner [33,34]; therefore, all measurements were made in the middle of the day, 4–8 h after light onset.

Electroretinography

Dark-adapted ERG recordings were obtained from anesthitized mice as described previously.[35] Briefly, mice were dark-adapted overnight. Mice were anesthetized with ketamine/xylazine (70/10 mg/kg). Topical 0.5% proparacaine HCL eye drops were applied, pupils were dilated with 1% tropicamide ophthalmic solution, and carboxymethylcellulose sodium eye drops were applied to keep the cornea moist. Body temperature was maintained at 37°C with a heating pad. Reference and ground electrodes were place in the cheek and tail. Dawson-Trick-Litzow (DTL) fiber recording electrodes were placed on the cornea.

Stimulus flashes were presented in a UTAS Big Shot Ganzfeld (LKC Technologies, Gaithersburg, MD). The flash duration was 20 μsec, and stimuli were presented in order of increasing intensity. As flash intensity increased, the interstimulus interval was progressively increased to maintain dark-adaptation.

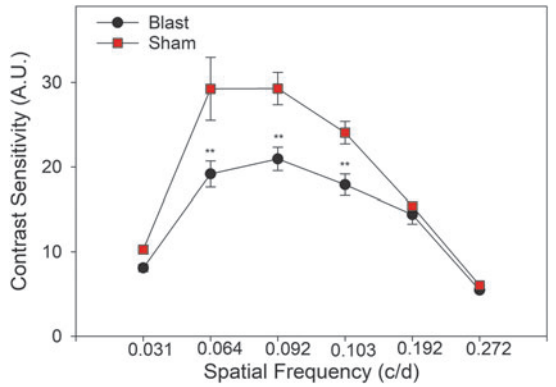

FIG. 1. Effect of ocular blast injury on contrast sensitivity functions. Contrast sensitivity functions were measured in sham mice and mice exposed to blast in the right eye by measuring the optomotor respose, as descried in Methods. Measurements in all animals began eight days after blast injury and were completed by 14 days after blast. $n = 8$/group. Blast significantly reduced contrast sensitivity at spatial frequencies of 0.064, 0.092, and 0.103 cycles/degree (c/d) (**$p < 0.01$).

Retinal histology

After mice were euthanized, superior was marked on the cornea using a cautery tool. Whole eyes were fixed in 2.5% glutaraldehyde in 0.1M cacodylate buffer for five days at 4°C, then washed twice with 0.1M cacodylate buffer. Cornea, lens, and iris were removed by dissection leaving a cornea flap on the superior side for orientation. The remaining posterior eye cups were stained with osmium tetroxide and embedded in plastic resin. They were sectioned at a thickness of 1 μm and stained with toluidine blue. Photomicrographs were generated in an area of superior retina centered at 800 μm above the optic nerve.

Confocal microscopy

Retinal flat mounts were imaged using a Nikon Eclipse C1 inverted confocal imaging system (Nikon Instruments, Melville, NY) to count putative RGCs in the Thy1-CFP reporter line. Samples were coded, and the microscopist was masked to the treatment.

Spectral domain optical coherence tomography (SD-OCT):

Mice were anesthetized with ketamine/xylazine. The SD-OCT imaging was performed on retinas of both eyes of mice using Phoenix Micron IV spectral-domain ophthalmic imaging system (Phoenix Research Labs, Pleasanton, CA). Proparacaine hydrochloride (0.5%) and topical tropicamide (1%; Akorn Inc.; Lake Forest, IL) were used to anesthetize the cornea and dilate the pupils, respectively. Corneal desiccation was prevented by applying topical GenTeal Lubricant Eye Gel (Novartis, East Hanover, NJ) during the procedure.

Mice were secured and scanned with the use of the animal imaging mount and rodent alignment stage. Fundus images were obtained with the StreamPix software. The SD-OCT images were taken with Micron OCT, restricted to retinal regions corresponding to a circle with a diameter of 0.57 mm centered on the optic nerve head (ONH) and full line scan of 1.8 mm. Retinal layer measurements were performed on the average of 50 scans of each retina using Adobe Photoshop CS6.

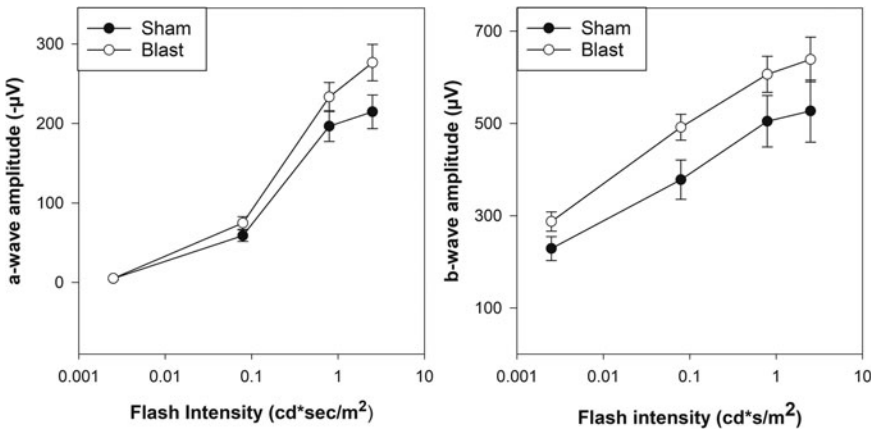

FIG. 2. Effect of ocular blast injury on dark-adapted electroretinogram (ERG) responses. Dark-adapted ERG responses were recorded eight weeks after exposure to blast. No significant differences were observed in a- or b-wave amplitudes, although there was a trend for higher b-wave amplitudes in the blast group. $n = 4$.

Statistics

Data are expressed as mean ± standard error of the mean, and were analyzed by Student *t* test for two groups and by one, two, or three-way analysis of variance (ANOVA), with a *post hoc* multiple comparison test (Student-Newman-Keuls or Holm-Sidak) where appropriate. All the statistical analyses were performed using SigmaPlot (Systat Software, Inc., San Jose, CA).

Results

Visual function and retinal damage after blast

We first examined contrast sensitivity of mice 1–2 weeks after exposure to blast using the optomotor response at multiple spatial frequencies (Fig. 1). In sham control mice, the peak contrast sensitivity was observed at 0.064 c/d, identical to that observed by Prusky and associates.[32] Contrast sensitivity was significantly reduced

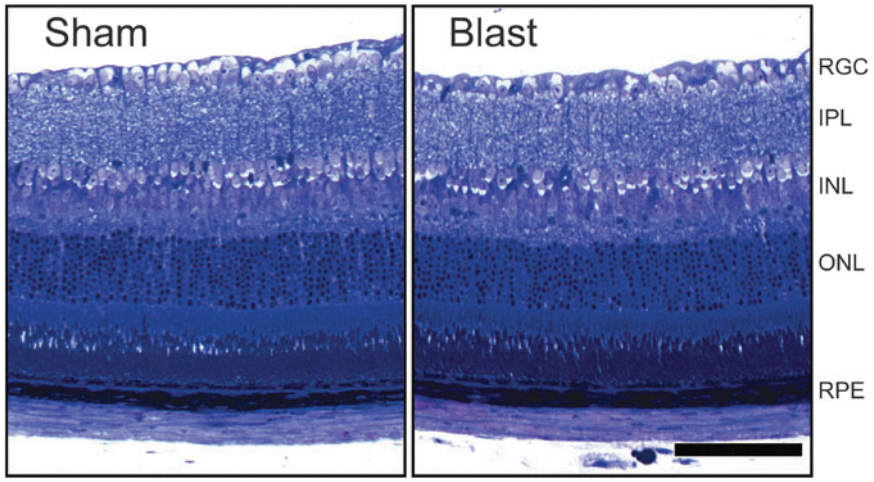

FIG. 3. Retinal histology after blast exposure. Representative 1 μm thick plastic sections of retina from sham and blast mice obtained two months after ocular blast injury showed thinner retina in blasted mice. Retinal ganglion cell (RGC) layer and inner plexiform layer (IPL) appear thinner in mice exposed to blast overpressure compared with sham mice. The other retinal layers appeared similar in both groups of mice. Photomicrographs were generated in an area of superior retina centered at 800 μm above the optic nerve. The scale bar is 100 μm. INL, inner nuclear layer; ONL, outer nuclear layer; RPE, retinal pigment epithelium.

($p < 0.01$) at spatial frequencies of 0.064, 0.092, and 0.103 c/d. The largest effect of blast was observed at a spatial frequency of 0.064 c/d, and this was used in all subsequent studies assessing the effects of HIOC on blast-induced disruption of visual contrast sensitivity (see below).

One week after blast, there was a small but significant decrease in visual acuity (spatial frequency thresholds: sham 0.386 ± 0.004 c/d; blast 0.365 ± 0.006; $N = 6$ $p < 0.02$). Scotopic ERG measurements seven weeks after blast showed no blast-induced decrements in a- or b-wave amplitudes, suggesting that photoreceptor and ON bipolar cell function were intact (Fig. 2); amplitudes were slightly higher in the mice exposed to blast.

Plastic sections of the retina two months after blast were prepared and stained with toluidine blue. Overall, retinas of the blasted mice appeared slightly thinner than sham control mice (Fig. 3). The photoreceptor layer was relatively preserved, consistent with the ERG results, whereas loss of RGCs and thinning of the inner plexiform layer was observed, suggesting that blast exposure affects RGCs in the retina (Fig. 3).

The number of CFP positive cells in flat mount retina preparations from sham and blast of Thy1-CFP mice were compared to calculate RGC death in the retina two months after ocular blast injury. Briefly, each retinal flat mount was divided into eight regions, as shown in Figure 4, such that regions 1 through 4 were close to the ONH and regions 5 through 8 were toward the periphery of each flat mount. Each region consisted of a ''cutbox'' that was $636.5\ \mu m \times 636.5\ \mu m$ in dimension and was prepared in Adobe Photoshop. The numbers of CFP positive cell bodies were counted using the ''count tool'' in Photoshop in each of the cutboxes.

Two months after exposure to blast, the numbers of CFP positive cells in central and peripheral retina of blasted mice were significantly reduced (Fig. 4; $p < 0.02$).

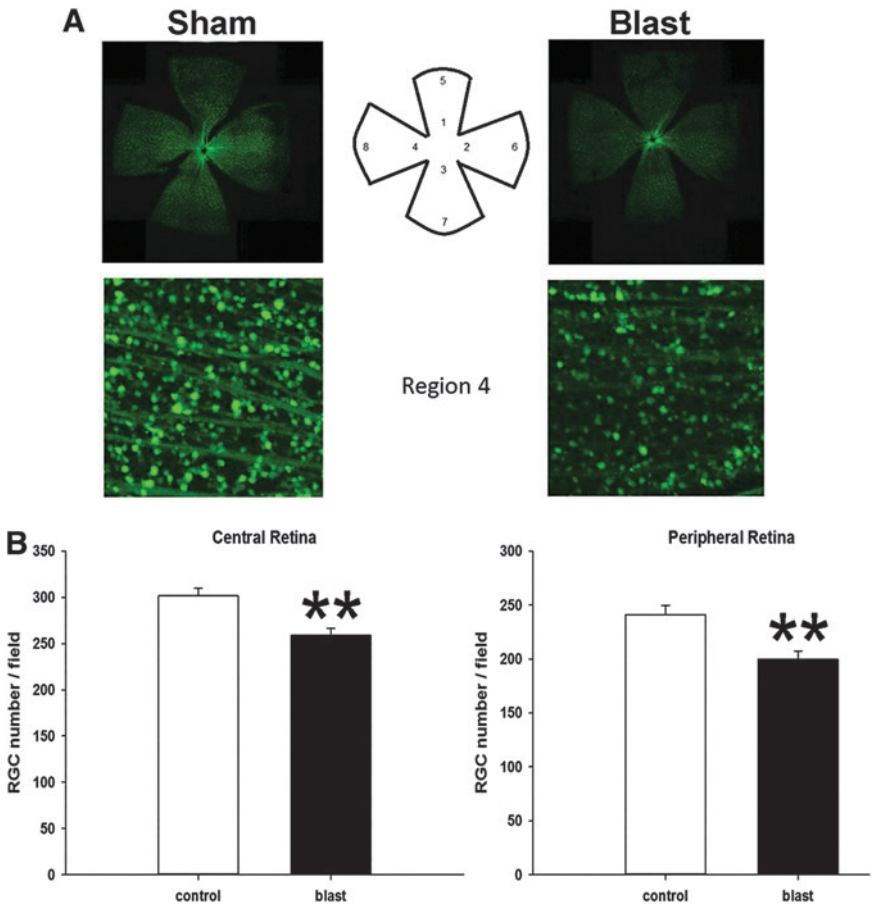

FIG. 4. Loss of retinal ganglion cells (RGCs) two months after blast. (**A**) Representative retinal flat mounts showing reduced fluorescent RGCs of Thy1-CFP (cyan fluorescent protein) mice after blast. (**B**) Cell counts from four 636.5 X 636.5 μm fields of both central and peripheral regions. A significant decrease in RGCs was observed in blasted animals two months post-blast (**$p < 0.02$) in both central and peripheral retina. Values for central retina are the mean of regions 1–4; those for peripheral retina are the mean of regions 5–8 ($n = 6$ mice/group).

Retinas of mice exposed to blast had 15% fewer CFP+ cells compared with sham controls. Collectively, our quantitative analysis suggests that ocular blast injury affects RGCs in the retina.

Neuroprotective effect of HIOC: dose-response

The efficacy of HIOC at different doses was tested to determine the optimal dose required for the neuroprotective effects of HIOC. Mice were injected IP with vehicle (10% DMSO), or different doses of HIOC (30 mg/kg, 60 mg/kg, and 100 mg/kg) immediately after blast to the right eye and once every 24 h for next six days. Contrast sensitivity and visual acuity of right eyes were significantly lower in vehicle-treated mice exposed to blast compared with the sham after one week ($p < 0.001$; Fig. 5 a,c).

Mice treated with 60 and 100 mg/kg HIOC showed significant improvement in visual function, with notably higher contrast sensitivity compared with the vehicle-treated mice one week after blast ($p < 0.05$). Visual acuity was also significantly reduced in all blast groups one week after the blast compared with sham. The HIOC (60 mg/kg) treatment significantly improved visual acuity compared with vehicle one week after blast ($p < 0.05$ vs. vehicle).

One month after blast, vehicle-treated mice continued to have lowest contrast sensitivity in their right eyes compared with sham (Fig. 5b,d). Mice treated with three different HIOC doses had significantly higher contrast sensitivity compared with vehicle-treated mice exposed to blast ($p < 0.001$ in 60 mg/kg; $p < 0.05$ in 30 mg/kg, and 100 mg/kg vs. vehicle). There was no significant difference between any of the tested HIOC doses.

Visual acuity results were similar to the contrast sensitivity one month after blast exposure. Vehicle-treated mice had the lowest visual acuity threshold whereas all HIOC treated groups had significantly higher visual acuity threshold than the vehicles ($p < 0.05$). Overall, HIOC mitigated decreased visual function until at least one month after blast at doses as low as 30 mg/kg when injected IP. The HIOC was injected at a dose of 40 mg/kg in subsequent experiments to ensure that enough HIOC was administered to observe any visual function rescue effects.

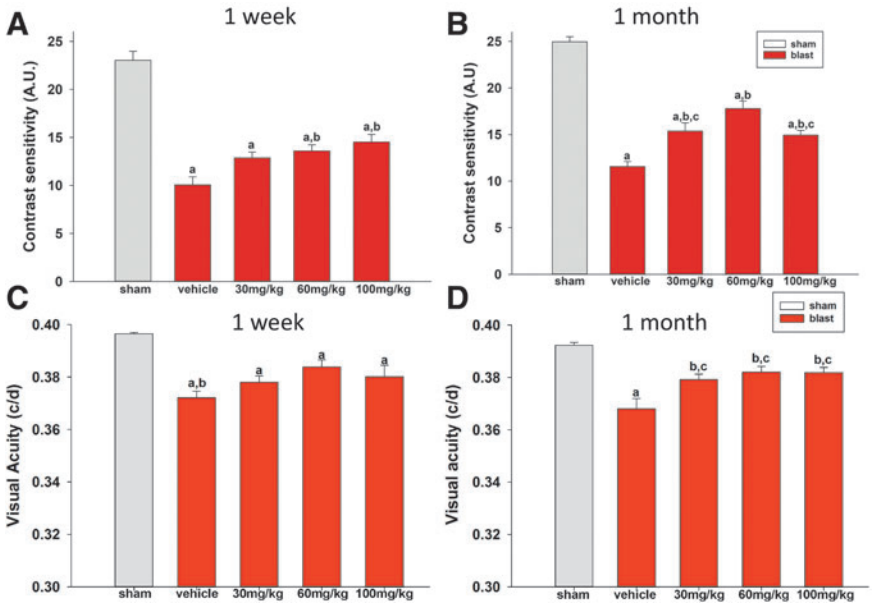

FIG. 5. Visual function in response to different N-[2-(5-hydroxy-1H-indol-3-yl)ethyl]-2-oxopiperidine-3-carboxamide (HIOC) dose treatment after blast. Mice treated with blast exposure had significantly reduced contrast sensitivity and visual acuity one week and one month after blast. Contrast sensitivity, measured at a spatial frequency of 0.064 cycles/degree (c/d), was significantly higher in 60 mg/kg and 100 mg/kg HIOC-treated mice compared with other groups one week after blast. Visual acuity at one week post-blast was significantly better versus vehicle-treated mice only in the 60 mg/kg group. One month after blast, both contrast sensitivity and visual acuity were improved at all HIOC doses relative to vehicle treated mice ($n = 6$ mice/group). (**A**) a) $p < 0.001$ vs. sham; b) $p < 0.05$ vs. vehicle. (**B**) a) $p < 0.001$ vs. sham; b) $p < 0.05$ vs. vehicle; c) $p < 0.05$ vs. 60 mg/kg; (**C**) a) $p < 0.05$ vs. sham; b) $p < 0.05$ vs. 60 mg/kg; (**D**) a) $p < 0.001$ vs. sham; b) $p < 0.05$ vs. sham; c) $p < 0.05$ vs. vehicle.

HIOC preserves visual function by activating TrkB

To determine whether HIOC mitigation of blast-induced vision loss was because of the activation of TrkB receptors, mice were treated with a selective TrkB receptor antagonist before HIOC treatment. Mice were pre-treated with N-[2-[[(Hexahydro-2-oxo-1H-azepin-3-yl) amino] carbonyl] phenyl] benzo[b]thiophene-2-carboxamide (ANA12), a selective TrkB antagonist,[36] 2.5 h before blast injury to the right eye. The HIOC or vehicle was administered initially15 min after the blast. Mice were treated with either ANA12, HIOC, or both for a total of seven consecutive days including the day of blast injury, with ANA12 administration preceding HIOC or vehicle by 2.5 h on each day.

When assessed one month after blast injury, contrast sensitivity and visual acuity were reduced in the vehicle-treated mice ($p < 0.001$ and $p < 0.05$, respectively) (Fig. 6). Treatment with HIOC (plus the vehicle for ANA-12) reduced the loss of contrast sensitivity ($p < 0.01$). Administration of ANA-12 alone had no effect on the blast-induced loss of contrast sensitivity, but completely blocked the effect of HIOC. The results support the hypothesis that HIOC mitigates blast-induced vision loss by activating TrkB.

Effective time frame to observe HIOC rescue effects after ocular blast injury

Mice were exposed to a single blast directed to their right eye. Mice received an initial injection of HIOC (40 mg/kg, IP) at various times before or after blast exposure: 30 min before blast, or 15 min, 1 h, 3 h, 24 h after blast. Vehicle was administered 30 min before blast for the vehicle-treated mice. Uninjured sham mice were treated with anesthesia only. The HIOC and vehicle were subsequently injected daily for an additional six days.

Contrast sensitivity and visual acuity were measured to test visual function one week and four months after blast (Fig. 7). Exposure to blast reduced contrast sensitivity, measured at a spatial frequency of 0.064 c/d, by 51% in the vehicle-treated mice at one week (Fig. 7a). The HIOC administered before blast injury partially reversed the loss of contrast sensitivity at one week ($p < 0.05$). The HIOC administered 15 min, 1 h, or 3 h after blast injury was as effective as the drug administered before injury; contrast sensitivity of those treated with HIOC before blast was not statistically different from contrast sensitivity of mice administered HIOC 15 min, 1 h, or 3 h after blast ($p > 0.2$). Mice who received the initial HIOC injection 24 h after blast showed no protective effect.

Visual acuity showed a trend for blast-induced reduction and a rescue by HIOC, but the effects were not statistically significant in this experiment one week after blast injury because of variability ($p = 0.16$, Fig. 7b).

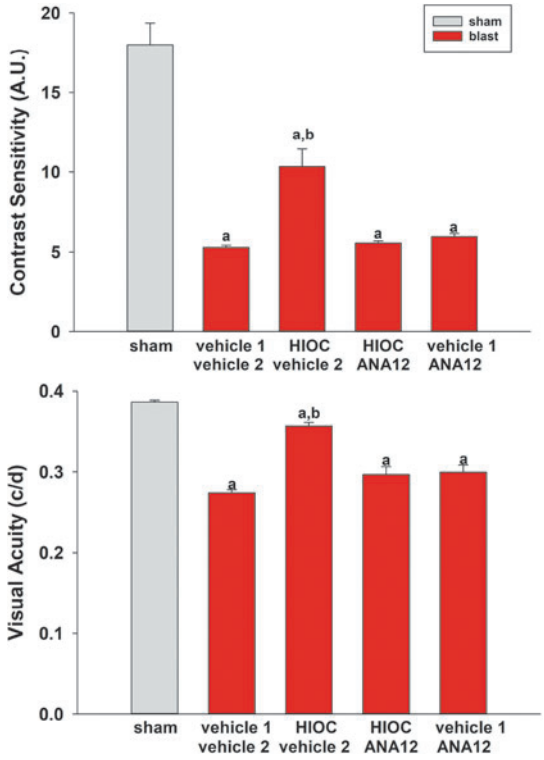

FIG. 6. The therapeutic effect of N-[2-(5-hydroxy-1H-indol-3-yl)ethyl]-2-oxopiperidine-3-carboxamide (HIOC) is blocked by tropomycin-related kinase B (TrkB) antagonist, N-[2-[[(Hexahydro-2-oxo-1H-azepin-3-yl) amino] carbonyl] phenyl] benzo[b]thiophene-2-carboxamide (ANA12). Mice were injected with ANA12 (2.5 h before blast), HIOC (15 min after blast) or both HIOC and ANA12; daily drug treatments continued for six days. Vehicle 1 refers to the vehicle for HIOC; vehicle 2 is the vehicle for ANA12. Contrast sensitivity, measured at 0.064 cycles/degree (c/d), and visual acuity were significantly reduced in vehicle-treated mice one month after blast. The HIOC reduced the blast-induced reduction in visual function, and this effect of HIOC was completely blocked by ANA12. (**A**) a) $p < 0.001$ vs. sham; b) $p < 0.05$ vs. HIOC; (**B**) a) $p < 0.001$ vs. sham; b) $p < 0.05$ vs. all other blast groups; ($n = 6$ mice/group).

Four months after blast injury, contrast sensitivity ($p < 0.001$) and visual acuity ($p < 0.001$) in the vehicle-treated mice were significantly reduced compared with sham controls (Fig. 7 c,d). The HIOC administered before blast injury completely reversed the loss of visual function at four months ($p < 0.001$). The HIOC administered 15 min, 1 h, or 3 h after blast injury was as effective

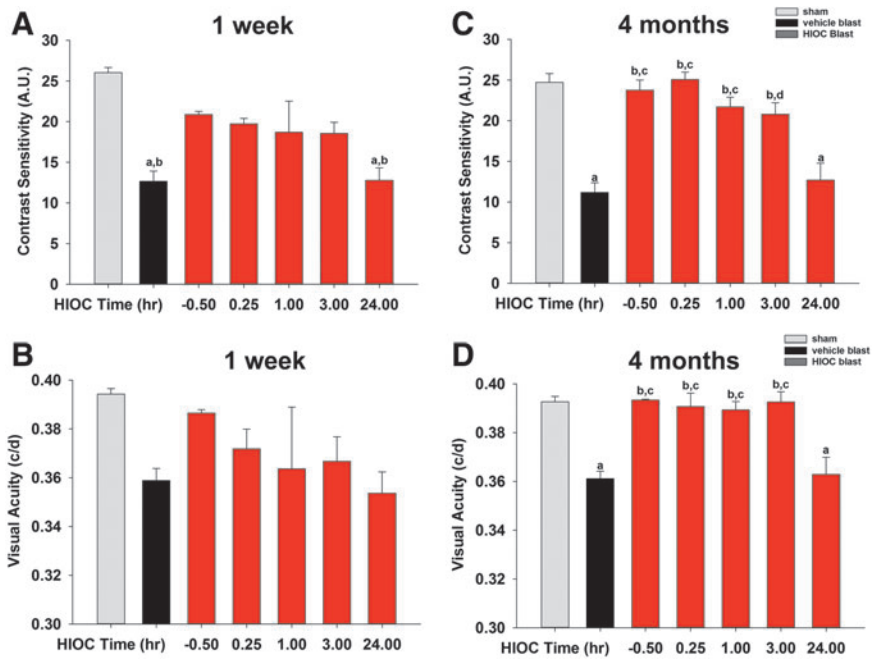

FIG. 7. Protective effects of N-[2-(5-hydroxy-1H-indol-3-yl)ethyl]-2-oxopiperidine-3-carboxamide (HIOC) injected before or after ocular blast injury. Contrast sensitivity was significantly reduced one week and four months after blast compared with sham and HIOC treated (40 mg/kg, IP, within 3 h post-blast) mice. Visual acuity was reduced four months after blast. "HIOC Time" refers to the time of drug administration relative to exposure to blast. (**A**) Contrast sensitivity at 0.064 cycles/degree: a) $p < 0.001$ vs. sham; b) $p < 0.05$ vs. HIOC (30 min before); (**B**) a) $p < 0.001$ vs. sham; b) $p < 0.001$ vs. vehicle; c) $p < 0.001$ vs. 24 h post; d) $p < 0.05$ vs. 24 h post; (**C**) no significant difference in visual acuity one week after blast; (**D**) a) $p < 0.001$ vs. sham; b) $p < 0.001$ vs. vehicle; c) $p < 0.001$ vs. 24 h post; $n = 6$ mice/group.

as the drug administered before blast; contrast sensitivity and visual acuity of mice treated with HIOC before blast were not statistically different from contrast sensitivity and visual acuity of mice administered HIOC 15 min, 1 h, or 3 h after blast ($p > 0.3$). As observed at one week post-blast, mice that received their initial injection of HIOC 24 h after blast showed no improvement in contrast sensitivity or visual acuity when assessed at four months.

These findings indicate that HIOC provides effective therapy for blast injury if treatment begins within 3 h of blast exposure, but not if treatment is delayed by one day. They also show that one week of HIOC treatment provides protection from vision loss that lasts in mice at least four months.

Effects of HIOC on RGC and NFL damage after blast injury

The SD-OCT measurements showed significantly reduced RGC and NFL thickness after one week in blast mice compared with sham (Fig. 8; $p < 0.01$). In mice treated with HIOC (40 mg/kg), there was significant preservation in RGC/NFL thickness compared with vehicle-treated mice ($p < 0.05$), demonstrating neuroprotective effects of HIOC in this blast model. No difference in photoreceptor layer thickness was observed at one week between any groups of mice (sham $100 \pm 0.5\ \mu$m; blast vehicle $99 \pm 0.8\ \mu$m; blast HIOC $100 \pm 0.8\ \mu$m).

Discussion

The major findings of this study are summarized: (1) Ocular blast injury results in inner retinal damage, particularly RGCs, resulting in loss of visual function; (2) HIOC treatment once a day for a week, with initial treatment within a defined time window after exposure to blast injury, mitigates vision loss for at least four months; (3) the effect of HIOC is mediated by activation of TrkB/BDNF receptors. Together, these findings suggest a potential therapeutic approach to preserve visual function after blast or other blunt force trauma to the eyes.

The RGC damage after exposure to ocular blast injury in our study is consistent with other reports.[10,11] The thinning of the RGC/NFL one week after ocular blast injury suggests an early onset of degeneration, which results in significantly fewer RGCs in mice exposed to blast

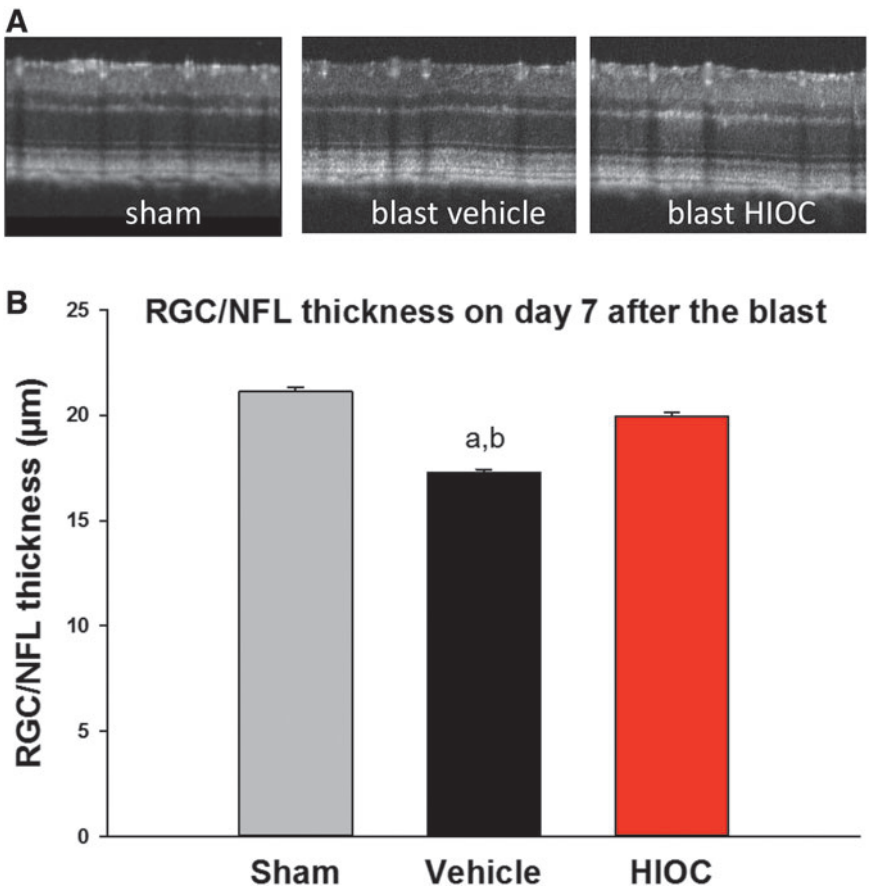

FIG. 8. Effect of blast exposure and N-[2-(5-hydroxy-1H-indol-3-yl)ethyl]-2-oxopiperidine-3-carboxamide (HIOC) on retinal ganglion cell/nerve fiber layer (RGC/NFL) thickness. (**A**) Representative spectral domain optical coherence tomography (SD-OCT) images from sham, vehicle blast, and HIOC blast treated mice. (**B**) SD-OCT measurements of RGC/NFL thickness showed significantly reduced thickness in vehicle-treated mice one week after blast; HIOC significantly mitigated RGC/NFL loss after blast. a) $p < 0.001$ vs. sham; b) $p < 0.05$ vs. HIOC; $n = 6$ mice/group.

compared with sham controls two months after injury. Decreases of contrast sensitivity and visual acuity also suggest that RGCs are primarily affected by blast injury under the conditions used in our experiments.

A decrease in contrast sensitivity, an indicator of ganglion cell function[37] in mice as early as one week after blast is consistent with RGCs being affected as a result of ocular blast injury, although the contrast deficit could have been because of outer retinal injury.[9] Moreover, we observed no decrease in ERG a- and b-wave amplitudes in response to blast overpressure, similar to the results of Bricker-Anthony and colleagues[9] and Allen and coworkers,[38] suggesting that the outer retina is not as severely affected as the RGCs under the conditions used in these experiments. Based on our data, drugs targeting RGCs in particular might offer a novel approach to new therapeutic tools to prevent vision loss after closed-globe ocular trauma.

N-Acetylserotonin, the immediate precursor of the hormone melatonin, is synthesized from serotonin by arylalkylamine *N*-acetyltransferase in the pineal gland and, to a lesser extent, in the retina.[39,40] In addition to its role as the melatonin precursor, *N*-acetylserotonin may have antioxidant properties that might afford a neuroprotective effect.[41] *N*-Acetylserotonin also activates the TrkB receptor, resulting in an antidepressant-like behavioral action, neuroprotection from excitotoxin-induced neuronal degeneration,[42] and increased neurogenesis.[26] These studies suggest that *N*-acetylserotonin is an endogenous neurotrophin-like compound. A limitation to *N*-acetylserotonin as a therapeutic agent is its short half-life after IP or intravenous injection.[25]

The HIOC is a structural analog of *N*-acetylserotonin that also activates TrkB.[25] When administered systemically, HIOC crosses the blood-retina and blood–brain barriers, has a significantly longer half-life than

N-acetylserotonin, and elicits a long-lasting activation of TrkB (>16 h) in the brain and retina.[25] Accordingly, systemic administration of HIOC mitigates light-induced retinal degeneration[25] and reduces neuronal death in the brain resulting from subarachnoid hemorrhage.[43]

In the current study, we found that HIOC administration protected against vision loss from ocular blast. Blast-induced decrements of both contrast sensitivity and visual acuity were reduced in HIOC-treated mice. The HIOC treatment effectively protected vision when the initial dose was administered up to 3 h after blast, but not if the initial treatment was delayed for 24 h. The rescue of visual function may be from a direct effect of HIOC on TrkB receptors on RGCs, because administration of the drug stimulates RGC TrkB phosphorylation.[25]

Analysis of the time course of vision loss and recovery with HIOC showed two trends. First, the loss of visual function was progressive; visual acuity deficits were not consistently statistically significant one week after blast exposure, but became highly significant one and four months after the traumatic insult. This result differs from a previous analysis of RGC function with the pattern electroretinogram (PERG), which showed a decrease in PERG amplitude at one week after blast, a recovery at four weeks, and then further decrease at 16 weeks.[44] It is unclear whether this reflects differences in the outcome measures (OMR vs. PERG) or the method of inducing trauma (focal ocular blast vs. an enclosed blast chamber in which the whole head of the mouse was exposed to the blast wave).

Second, the improvement in visual function produced by HIOC gradually increased over time, such that only partial recovery was observed at one week or one month, but near total recovery by four months. This occurred even though drug administration was terminated one week after exposure to the blast wave. The mechanism of this progressive recovery is unknown. A reduction of the initial number of retinal ganglion cells damaged during the first week after blast in HIOC-treated mice, however, may have resulted in enhanced sprouting of axon terminals resulting in gradual recovery of function. Alternatively, the mechanism may be related to recovery of normal neuronal function in the retina and/or brain.

It is possible that our data underestimate the amount of RGC loss after blast. Raymond and associates[45] reported that some of the CFP+ cells in the GCL are amacrine cells. These cells are less fluorescent than the RGCs. We counted all fluorescent cells in the flat mount samples. Thus, if blast selectively affected RGCs, more than 15% of RGCs may have been lost after blast.

Although the blast was directed at the eye, we cannot exclude the possibility that damage in the brain contributes to vision loss. In this regard, it is noteworthy that HIOC crosses the blood–brain barrier, as well as the blood-retina barrier, and has neuroprotective effects in the brain.[25] Thus, it is possible that the functional improvement seen with HIOC administration involves effects on the brain, as well as on the retina.

Conclusion

Our study suggests that HIOC or similar small molecule activators of TrkB may be effective treatments for preserving vision following closed-globe ocular trauma.

Acknowledgments

Opinions, interpretations, conclusions, and recommendations are those of the authors and are not necssarily endorsed by the Department of Defense or other funding agencies. The authors thank Julien Brock for excellent technical assistance.

Funding Information

This study was supported by the Department of Defense, through the US Army Medical Research and Development Command under Awards W81XWH-18-1-0700, W81XWH-12-1-0436, and W81XWH12-1-0255 (PMI, EEG), by the NIH P30EY06360 (Emory Vision Core, PMI) and R01EY028859 (JHB), by the VA via I01RX002806 (JHB/PMI), by unrestricted funds from Research to Prevent Blindness, and by a gift from the Abraham J. and Phyllis Katz Foundation (JHB/PMI).

Author Disclosure Statement

No competing financial interests exist.

References

1. Chan, R.K., Siller-Jackson, A., Verrett, A.J., Wu, J., and Hale, RG. (2012). Ten years of war: a characterization of craniomaxillofacial injuries incurred during operations Enduring Freedom and Iraqi Freedom. J. Trauma Acute Care Surg. 73, Suppl. 5, S453–S458.
2. Weichel, E.D., and Colyer, M.H. (2008). Combat ocular trauma and systemic injury. Curr. Opin. Ophthalmol. 19, 519–525.
3. Cockerham, G.C., Goodrich, G.L., Weichel, E.D., Orcutt, J.C., Rizzo, J.F. Bower, K.S., and Schuchard, R.A. (2009). Eye and visual function in traumatic brain injury. J. Rehabil. Res. Devel. 46, 811–818.
4. Sherwood, D,, Sponsel, W.E., Lund, B.J., Gray, W., Watson, R., Groth, S.L., Thoe, K., Glickman, D., and Reilly, M.A. (2014). Anatomical manifestations of primary blast ocular trauma observed in a postmortem porcine model. Invest. Ophthalmol. Vis. Sci. 55, 1124–1132.
5. Ferrari, L.R. (1996). The injured eye. Anesthesiol. Clin. North Am. 14, 125–150.
6. Podbielska, M., Das, A., Smith, A.W., Chauhan, A., Ray, S.K., Inoue, J. Azuma, M., Nozaki, K, Hogan, E.L., and Banik, N.L. (2016). Neuron-microglia interaction induced bi-directional cytotoxicity associated with calpain activation. J. Neurochem. 139, 440–455.
7. Levin, L.A., Beck, R.W., Joseph, M.P., Seiff, S., and Kraker, R. (1999). The treatment of traumatic optic neuropathy: the International Optic Nerve Trauma Study. Ophthalmology 106, 1268–1277.
8. McClenaghan, F.C., Ezra, D.G., and Holmes, S.B. (2011). Mechanisms and management of vision loss following orbital and facial trauma. Curr. Opin. Ophthalmol. 22, 426–431.
9. Bricker-Anthony, C., Hines-Beard, J., and Rex, T.S. (2014). Molecular changes and vision loss in a mouse model of closed-globe blast trauma. Invest. Ophthalmol. Vis. Sci. 55, 4853–4862.
10. Mohan, K., Kecova, H., Hernandez-Merino, E., Kardon, R.H., and Harper, M.M. (2013). Retinal ganglion cell damage in an experimental rodent model of blast-mediated traumatic brain injury. Invest. Ophthalmol. Vis. Sci. 54, 3440–3450.
11. DeMar, J., Sharrow, K., Hill, M., Berman, J., Oliver, T., and Long, J. (2016). Effects of primary blast overpressure on retina and optic tract in rats. Front. Neurol. 7, 59.

12. Zou, Y.Y., Kan, E.M., Lu, J., Ng, K.C., Tan, M.H., Yao, L., and Ling, E.A. (2013). Primary blast injury-induced lesions in the retina of adult rats. J. Neuroinflammation 10, 849.
13. Jones, K., Choi, J.H., Sponsel, W.E., Gray, W., Groth, S.L., Glickman, R.D., Lund, B.J., and Reilly, M.A. (2016). Low-level primary blast causes acute ocular trauma in rabbits. J. Neurotrauma 33, 1194–1201.
14. Hennigan, A,, O'Callaghan, R.M., and Kelly, A,M. (2007). Neurotrophins and their receptors: roles in plasticity, neurodegeneration and neuroprotection. Biochem. Soc. Trans. 35, 424–427.
15. Mocchetti, I., and Bachis, A. (2004). Brain-derived neurotrophic factor activation of TrkB protects neurons from HIV-1/gp120-induced cell death. Crit. Rev. Neurobiol. 16, 51–57.
16. Wu D. (2005). Neuroprotection in experimental stroke with targeted neurotrophins. NeuroRx 2, 120–128.
17. Mansour-Robaey, S., Clarke, D.B., Wang, Y.C., Bray, GM.., and Aguayo, A.J. (1994). Effects of ocular injury and administration of brain-derived neurotrophic factor on survival and regrowth of axotomized retinal ganglion cells. Proc. Natl. Acad. Sci. U.S.A. 91, 1632–1636.
18. Weber, A.J., Viswanathan, S., Ramanathan, C., and Harman, C.D. (2010). Combined application of BDNF to the eye and brain enhances ganglion cell survival and function in the cat after optic nerve injury. Invest. Ophthalmol. Vis. Sci. 51, 327–334.
19. Gauthier, R., Joly, S., Pernet, V., Lachapelle, P., and Di Polo, A. (2005). Brain-derived neurotrophic factor gene delivery to muller glia preserves structure and function of light-damaged photoreceptors. Invest. Ophthalmol. Vis. Sci. 46, 3383–3392.
20. LaVail, M.M., Yasumura, D., Matthes, M.T., Lau-Villacorta, C., Unoki, K., Sung, C.H., and Steinberg, R.H.. (1998). Protection of mouse photoreceptors by survival factors in retinal degenerations. Invest. Ophthalmol. Vis. Sci. 39, 592–602.
21. Huang, E.J., and Reichardt, L.F. (2003). Trk receptors: roles in neuronal signal transduction. Annu. Rev. Biochem. 72, 609–642.
22. Klein, R., Nanduri, V., Jing, S.A., Lamballe, F., Tapley, P., Bryant, S., Cordon-Cardo, C., Jones, K.R., Reichardt, L.F., and Barbacid, M. (1991). The trkB tyrosine protein kinase is a receptor for brain-derived neurotrophic factor and neurotrophin-3. Cell 66, 395–403.
23. Mitre, M., Mariga, A., and Chao, M.V. (2017). Neurotrophin signalling: novel insights into mechanisms and pathophysiology. Clin. Sci. (Lond) 131, 13-–23.
24. Iuvone, P.M., Boatright, J.H., Tosini, G., and Ye, K. (2014). N-acetylserotonin: circadian activation of the BDNF receptor and neuroprotection in the retina and brain. Adv .Exp. Med. Biol. 801, 765–771.
25. Shen, J., Ghai, K., Sompol, P., Liu, X., Cao, X., Iuvone, P.M., and Ye, K. (2012). N-acetyl serotonin derivatives as potent neuroprotectants for retinas. Proc. Natl. Acad. Sci. U.S.A. 109, 3540–3545.
26. Sompol, P., Liu, X., Baba, K., Paul, K.N., Tosini, G., Iuvone, P.M., and Ye, K. (2011). N-acetylserotonin promotes hippocampal neuroprogenitor cell proliferation in sleep-deprived mice. Proc. Natl. Acad. Sci. U.S.A. 108, 8844–8849.
27. Feng, G., Mellor, R.H., Bernstein, M., Keller-Peck, C., Nguyen, Q.T., Wallace, M., Nerbonne, J.M., Lichtman, J.W., ad Sanes, J.R. (2000). Imaging neuronal subsets in transgenic mice expressing multiple spectral variants of GFP. Neuron 28, 41–51.
28. Hines-Beard, J., Marchetta, J., Gordon, S., Chaum, E., Geisert, E.E., and Rex, T.S. (2012). A mouse model of ocular blast injury that induces closed globe anterior and posterior pole damage. Exp. Eye Res. 99, 63–70.
29. Struebing, F.L., King, R., Li, Y., Chrenek, M.A., Lyuboslavsky, P.N., Sidhu, C.S., Luvone, P.M., and Geisert, E.E. (2018). Transcriptional changes in the mouse retina after ocular blast injury: a role for the immune system. J. Neurotrauma 35, 118–129.
30. Setterholm, N.A., McDonald, F.E., Boatright, J.H., and Iuvone, P.M. (2015). Gram-scale, chemoselective synthesis of N-[2-(5-hydroxy-1H-indol-3-yl)ethyl]-2-oxopiperidine-3-carboxamide (HIOC). Tetrahedron Lett. 56, 3413–3415.
31. Douglas, R.M., Alam, N.M., Silver, B.D., McGill, T.J., Tschetter, W.W., and Prusky, G.T. (2005). Independent visual threshold measurements in the two eyes of freely moving rats and mice using a virtual-reality optokinetic system. Vis. Neurosci. 22, 677–684.
32. Prusky, G.T., Alam, N.M., Beekman, S., and Douglas, R.M. (2004). Rapid quantification of adult and developing mouse spatial vision using a virtual optomotor system. Invest. Ophthalmol. Vis. Sci. 45, 4611–4616.
33. Hwang, C.K., Chaurasia, S.S., Jackson, C.R., Chan, G.C., Storm, D.R., and Iuvone, P.M. (2013). Circadian rhythm of contrast sensitivity is regulated by a dopamine-neuronal PAS-domain protein 2-adenylyl cyclase 1 signaling pathway in retinal ganglion cells. J. Neurosci. 33, 14989–14997.
34. Jackson, C.R., Ruan, G.X., Aseem, F., Abey, J., Gamble, K., Stanwood, G., Palmiter, R.D., Iuvone, P.M., and McMahon, D.G. (2012). Retinal dopamine mediates multiple dimensions of light-adapted vision. J. Neurosci. 32, 9359–9368.
35. Baba, K., Piano, I., Lyuboslavsky, P., Chrenek, M.A., Sellers, J.T., Zhang, S., Gargini, C., He, L., Tosini, G., and Iuvone, P.M. (2018). Removal of clock gene Bmal1 from the retina affects retinal development and accelerates cone photoreceptor degeneration during aging. Proc, Natl. Acad. Sci. U. S. A. 115, 13099–13104.
36. Cazorla, M., Premont, J., Mann, A., Girard, N., Kellendonk, C., and Rognan, D. (2011). Identification of a low-molecular weight TrkB antagonist with anxiolytic and antidepressant activity in mice. J. Clin. Invest. 121, 1846–1857.
37. Field, D.T., Bell, L., Mount, S.W,. Williams, C.M., and Butler, L.T. (2014). Chapter 41. Flavonoids and visual function: observations and hypotheses A2. In: Preedy, V.R. (ed). *Handbook of Nutrition, Diet and the Eye.* San Diego, Academic Press; pp. 403–411.
38. Allen, R.S. Motz, C.T., Feola, A., Chesler, K.C., Haider, R., Ramachandra Rao, S., Skelton, L.A., Fliesler, S.J., and Pardue, M.T. (2018). Long-term functional and structural consequences of primary blast overpressure to the eye. J. Neurotrauma 35, 2104–2116.
39. Iuvone, P.M., Tosini, G., Pozdeyev, N., Haque, R., Klein, D.C., and Chaurasia, S.S. (2005). Circadian clocks, clock networks, arylalkylamine N-acetyltransferase, and melatonin in the retina. Prog. Retin. Eye Res. 24, 433–456.
40. Klein, D.C., Coon, S.L., Roseboom, P.H., Weller, J.L., Bernard, M., Gastel, J.A., Zatz, M., Rodriguez, I.R., Begey, V., Falcon, J., Cahill, G.M., Cassone, V.M., and Baler, R. (1997). The melatonin rhythm-generating enzyme: molecular regulation of serotonin N-acetyltransferase in the pineal gland. Recent Prog. Horm. Res. 52, 307–357.
41. Oxenkrug G. (2005). Antioxidant effects of N-acetylserotonin: possible mechanisms and clinical implications. Ann. N.Y. Acad. Sci. 1053, 334–347.
42. Jang, S.W., Liu, X., Yepes, M., Shepherd, K.R., Miller, G.W., Liu, Y., Wilson, W.D., Xiao, G., Blanchi, B., Sun, Y.E., and Ye, K. (2010). A selective TrkB agonist with potent neurotrophic activities by 7,8-dihydroxyflavone. Proc. Natl. Acad. Sci. U.S.A. 107, 2687–2692.
43. Tang, J., Hu, Q., Chen, Y., Liu, F., Zheng, Y., Tang, J., Zhang, J., and Zhang, J.H. (2015). Neuroprotective role of an N-acetyl serotonin derivative via activation of tropomyosin-related kinase receptor B after subarachnoid hemorrhage in a rat model. Neurobiol. Dis. 78, 126–133.
44. Dutca, L.M., Stasheff, S.F., Hedberg-Buenz, A., Rudd, D.S., Batra, N., Blodi, F.R., Yorek, M.S., Yin, T., Shankar, M., Herlein, J.A., Naidoo, J., Morlock, L., Williams, N., Kardon, R.H., Anderson, M.G., Pieper, A.A., and Harper, M.M. (2014). Early detection of subclinical visual damage after blast-mediated TBI enables prevention of chronic visual deficit by treatment with P7C3-S243. Invest. Ophthalmol. Vis. Sci. 55, 8330–8341.
45. Raymond, I.D., Vila, A., Huynh, U.C., and Brecha, N.C. (2008). Cyan fluorescent protein expression in ganglion and amacrine cells in a thy1-CFP transgenic mouse retina. Mol. Vis. 14, 1559–1574.

OPEN ACCESS
ARVO Annual Meeting Abstract | June 2022

2-Fluoro-N-(2-(5-hydroxy-1H-indol-3-yl)ethyl)nicotinamide (HIFN) protects against vision loss from closed-globe ocular trauma by activating tropomyosin-related kinase B (TrkB)

Shweta Modgil; Christopher L Walker; Frank E McDonald; P. Michael Iuvone

+ Author Affiliations & Notes

Investigative Ophthalmology & Visual Science June 2022, Vol.63, 1485. doi:

Abstract

Purpose : A small molecule activator of TrkB, HIOC, has been shown to protect against vision loss following ocular blast injury (Dhakal et al, J Neurotrauma 2021;38:2896). In this study, we assessed the protective effects of a fluoropyridine analog of HIOC.

Methods : Using HIOC as a lead structure, an analog (HIFN) containing fluorine substituted pyridine was synthesized. Adult male C57BL/6J mice were subjected to blast overpressure injury at ~20psi. Within 30 minutes of blast, animals were administered intraperitoneally either vehicle, HIFN or HIOC (40mg/kg). The treatment was continued for another 6 days. Contrast sensitivity at a spatial frequency of 0.064c/d and visual acuity (spatial frequency threshold) were measured using the optomotor response. Scotopic electroretinogram (ERG) and pattern ERG (spatial frequency of 0.155 c/d, 2.1 contrast reversal/sec and mean luminance of 50cd/m^2) were recorded. TrkB activation was assessed by western blot analysis of TrkB phosphorylation. Animals were administered with TrkB specific inhibitor, ANA-12 (0.5mg/kg), 2.5 h prior to treatment with compound.

Results : HIOC and HIFN both reduced the visual acuity ($p \leq 0.05$ *vs* Blast-Veh) and contrast sensitivity deficits after blast ($p \leq 0.05$ *vs* Blast-Veh). The protection of contrast sensitivity afforded by HIFN was better than that by HIOC at 7-week post blast ($p \leq 0.05$). No effects of

blast, HIFN, or HIOC were observed in the scotopic ERG a-wave or b-wave amplitudes. At 8-week post blast there was a significant decline in P1 and N2 wave amplitude of pERG in Blast-Veh group ($p \leq 0.001$). HIFN and HIOC treatment reduced the decline in P1 amplitude ($p \leq 0.05$ *vs* Blast-Veh). HIFN and HIOC showed a trend to increase the N2 amplitude compared to vehicle, but the effects were not statistically significant ($p=0.06$ *vs* Blast-Veh). HIFN activated TrkB at a concentration of 10 nM in NIH/3T3 cells expressing human TrkB. The TrkB inhibitor, ANA-12, blocked the protective effects exhibited by HIFN and HIOC in blast animals.

Conclusions : HIFN protects against blast-induced vision loss and retinal ganglion cell damage, as assessed by pERG. HIFN appears to preserve contrast sensitivity better than HIOC, although this needs to be assessed at different drug doses. The protective effects of HIFN are due to activation of TrkB receptor.

This abstract was presented at the 2022 ARVO Annual Meeting, held in Denver, CO, May 1-4, 2022, and virtually.

Introduction: Exposure to repetitive brain trauma has been associated with perivascular astrocytic tau pathology, which may contribute to neurodegeneration, though the mechanisms governing astrocytic tau accumulation are unclear. These studies examined the influence of repetitive mild traumatic brain injury (r-mTBI) and ApoE genotype on the interactions between astrocytes and extracellular tau.

Aims: 1) examine the mechanisms through which astrocytes process and/or eliminate tau, and 2) interrogate the effect of ApoE genotype and r-mTBI on these processes.

Methods: Brain injuries were administered to ApoE-targeted replacement mice ($n=8$ per group) 2 times per week for 12 weeks using a closed head injury model, and astrocytes were isolated 6 months post r-mTBI and exposed to exogenous tau.

Results: Tau accumulation was elevated by 2.3-fold ($p<0.0001$) in ApoE4 astrocytes exposed to r-mTBI compared to r-sham, whereas ApoE2 and ApoE3 astrocytes showed no difference in tau accumulation between injury groups. Specifically, ApoE4 astrocytes demonstrated a 25% increase ($p<0.05$) in tau colocalization with early endosomes, but a 50% reduction ($p<0.0001$) in tau colocalization with recycling endosomes, relative to other ApoE isoforms. Moreover, astrocyte secretion of tau over 1 hour was diminished by 4-fold ($p<0.0001$) following pharmacological inhibition of astrocyte exosome biogenesis.

Conclusion: These studies indicate astrocytes rapidly process and release tau under physiological conditions, but these processes become dysfunctional following r-mTBI, and are further exacerbated by the ApoE4 isoform, leading to astrocytic tau accumulation.

Keywords: Astrocyte, Neurodegeneration, Concussion/mTBI, Chronic Traumatic Encephalopathy

P215

DEVELOPING A MOUSE MODEL OF SPINAL CORD INJURY INDUCED BOWEL DYSFUNCTION

Mrs. Olivia Wireman[1], William, B. Bailey, Felicia Marino, Dr. John Gensel
[1]*University Of Kentucky, Lexington KY, United States*

Bowel dysfunction is one of the most prevalent and life-impacting comorbidities associated with spinal cord injury (SCI) with no long-term treatment available. The extent to which SCI-induced changes in the colon (e.g. inflammation, fibrosis, and reduced enteric neuron density) cause progressive dysfunction is understudied. There remains a significant unmet need to develop strategies to prevent or reverse bowel dysfunction after SCI. Previous studies have modeled chronic constipation after SCI in rats, however, mouse models of bowel dysfunction after SCI are less prevalent. We hypothesized that a T3 spinal transection would induce chronic functional bowel deficits coincident with colon pathology. Functional bowel deficits were examined through quantification of total transit time (TTT) and fecal pellet counts in the colon to model constipation and potential fecal impaction, respectively. TTT was significantly decreased by 3 days post injury (dpi) in animals receiving SCI compared to sham (laminectomy) injuries. Chronically, at 21 dpi, total fecal pellet count increased in SCI animals compared to those receiving sham injury. Chronic functional deficits measured by fecal pellet count and the presence of fibrosis are consistent with our hypothesis that T3 transection causes chronic bowel dysfunction in mice. Establishing this mouse model will enable further interrogation of cell-type specific responses and signaling pathways using transgenic models. Determining the extent to which SCI causes pathophysiological changes to the bowel will help develop therapies to improve the lives of individuals with SCI.

Keywords: Secondary Injury, Cell Death

P216

A NOVEL TROPOMYOSIN-RELATED KINASE-B (TRKB) RECEPTOR AGONIST PREVENTS VISION LOSS AFTER BLAST OVERPRESSURE INJURY

Dr. Shweta Modgil[1], Dr. L. Walker.C.[2], Dr. E. McDonald.F.[2], Dr. M. Iuvone.P.[1]
[1]*Department of Ophthalmology, School of Medicine, Emory University,Atlanta, Atlanta GA, United States,* [2]*Department of Chemistry, Emory University, Atlanta, Atlanta GA, United States*

Background: A small synthetic molecule, HIOC, was previously shown to effectively activate TrkB receptor and provide protection against ocular blast injury. In the current study, we used HIOC as a lead compound to develop novel TrkB activators and assess their efficacy in reducing ocular trauma-induced visual dysfunction. 2-Fluoro-N-(2-(5-hydroxy-1H-indol-3-yl)ethyl)nicotinamide (HIFN), a fluoropyridine analog of HIOC showed better TrkB phosphorylation compared to HIOC in culture and in-vivo studies.

Methods: HIOC derivatives were synthesized and tested in NIH-3T3-TrkB cells to screen promising TrkB activators using western blot analysis. Potential analogs were tested in C57BL/6J mice subjected to blast overpressure injury (20psi). Animals were treated with analogs 30-minute following blast and treatment was continued for another 6 days. Optomotor responses (contrast sensitivity and visual acuity) and pattern electroretinography (pERG) were used to assess visual and retinal ganglion cell function. ANA-12 (0.5mg/kg) was administered to animals 2.5 h prior to treatment with compound to inhibit TrkB activation.

Results: HIFN (10nM) elicited better TrkB phosphorylation than HIOC in culture and was effective in preserving visual acuity ($p\leq0.05$ vs Blast-Veh) and contrast sensitivity post ocular blast ($p\leq0.05$ vs Blast-Veh). HIFN was better than HIOC in preventing contrast sensitivity loss following blast ($p\leq0.05$). Treatment with HIFN also prevented the decline in the pERG P1 ($p\leq0.05$ vs Blast-Veh) and N2 amplitude ($p=0.06$ vs Blast-Veh) compared to vehicle. The TrkB inhibitor, ANA-12, prevented TrkB activation by HIFN in culture and ameliorated the protective effects exhibited in blast animals.

Conclusion: HIFN protects against blast-induced vision loss through activation of TrkB receptor.

Keywords: Blast, Receptor Mediated/Signaling

P217

THE INFLUENCE OF AGE ON ASTROCYTE AND MICROGLIAL NEUROIMMUNE RESPONSES AFTER TBI

Dr. Bevan Main[1], Alex Harvey[1], Ruchelle Buenaventura[1], Dr. Mark Burns[1]
[1]*Georgetown University, Washington DC, United States*

Background: Traumatic Brain Injury (TBI) is a major cause of disability and mortality, particularly among young adults and the elderly. Alongside age, neuroinflammation plays a key role in contributing to negative outcomes after TBI. Here, we explored the bi-directional crosstalk between astrocytes and microglia and how they contribute to age related TBI-induced neuroinflammatory responses.

In Q175 mice's striatum, we found no difference in ROS levels, while GSH levels were reduced at 8 m ($p < 0.05$), SOD2 expression was reduced at 4 m and increased at 8 m ($p < 0.05$), and UCP4 expression was reduced at both 4 and 8 m ($p < 0.05$). In Q175 mice's cortex, we observed reduced ROS levels at 8 m ($p < 0.01$), no difference in GSH levels, an increase in SOD2 expression at 8 m ($p < 0.05$), and an increase in UCP4 expression at 4 m and a reduction at 8 m ($p < 0.05$). Thus, while ROS levels are mostly maintained, evidence of oxidative stress is shown in the striatum of HD mice were UCP4 and SOD2 expression and GSH levels are modified. Cortex, which presents a later onset of the disease, started to exhibit some of these alterations at 8m. Mechanisms involved in oxidative stress in HD are largely unexplored and could represent targets for treating HD.

WTH10-14 | A novel tropomyosin-related kinase-B (TrkB) receptor activator: HIFN (2-fluoro-N-(2-(5-hydroxy-1H-indol-3-yl) ethyl)nicotinamide

Shweta Modgil[1], Christopher Walker[2], Frank McDonald[2], Michael Iuvone[1]

[1]*Emory University, Department of Opthalmology, Atlanta, USA;* [2]*Emory University, Department of Chemistry, Atlanta, USA*

Purpose: Our lab has previously reported a synthetic molecule, HIOC, could activate TrkB receptor and prevent vision loss from ocular trauma or phototoxic injury. In the present study we synthesized and tested novel HIOC analogs that could effectively activate TrkB receptor with greater potency.

Methods: Using HIOC as a lead compound, over 20 different analogs were synthesized. In preliminary screening for TrkB activation, these compounds (10 nM) were tested in NIH-3T3-TrkB cells and primary cortical neurons using western blot. Promising TrkB activators were further tested for protection against blast overpressure injury (20 psi) in C57BL/6J mice. Animals received analog (40 mg/kg) or vehicle, 30 min after blast and treatment was continued for another 6 days. Visual function (contrast sensitivity and visual acuity) and retinal function tests [scotopic ERG and pattern ERG (pERG)] were used to assess vision. A TrkB antagonist, ANA-12 (0.5 mg/kg), was administered to animals 2.5 h prior to treatment with TrkB activator to test specificity.

Results: A fluorine substituted pyridine analog (HIFN) showed better TrkB activation than the parent compound HIOC. HIFN prevented the deficit in visual acuity ($p \leq 0.05$) and contrast sensitivity after ocular blast ($p \leq 0.05$). HIFN proved better than HIOC in preserving contrast sensitivity in animals at 7-week post blast ($p \leq 0.05$). Treatment also prevented the decline in the pERG P1 amplitude ($p \leq 0.05$) and N2 amplitude ($p = 0.06$). ANA-12 (TrkB inhibitor) blocked TrkB activation by HIFN and prevented the protective effects in blast animals. Dose response studies using different HIFN concentrations (0–100 mg/kg) were carried out. Dose dependent rescue of visual function deficit was seen reaching significant levels at dose of 30 mg/kg for contrast sensitivity ($p \leq 0.0001$) and 10 mg/kg ($p \leq 0.05$) for visual acuity. At a dose of 30 mg/kg, HIFN also prevented ($p \leq 0.05$) the decline in retinal ganglion cell function, assessed by pERG.

Conclusion: HIFN activates TrkB receptor and protects against trauma-induced vision loss.

WTH10-15 | Ethinyl esrtadiol and levonorgestrel improves spatial memory and induces neurodegeneration in the limbic system of Wistar rats

Agnes Nwakanma[1], Mokutima Eluwa[2], Moses Ekong[3], Chukwuebuka Elemuo[1]

[1]*Chukwuemeka Odumegwu Ojukwu University, Human Anatomy, Ihiala, Nigeria;* [2]*University of Calabar, Anatomical Sciences, Calabar, Nigeria;* [3]*University of Uyo, Human Anatomy, Uyo, Nigeria*

Oral contraceptives have gained global publicity. Inconsistent reports on the neurological impact of oral contraceptives necessitated the study on the effect of oral contraceptives on the limbic system. Twenty four adult female wistar rats weighing 180–220 g were divided into four groups designated A, B, C, and D. Group A was the control and did not receive any treatment, Groups B, C, and D were treated with combined oral contraceptives containing 0.002 mg/kg levonorgestrel and 0.0043 mg/kg estradiol for 21, 42 and 63 days respectively via orogastric tube. The animals were exposed to Morris' water maze after 24 h of the last administration for each group. Blood was collected for serum estimation of serotonin, malondialdehyde, alpha feto protein and cortisol levels. All brains were perfused fixed weighed and post fixed in 10% buffered formalin. The hypothalamus, hippocampus and amygdala were dissected and processed for histological studies using Hematoxylin and eosin method, cresyl fast violet method for Nissl substance and immunolabeled for Glial fibrillary acidic protein and neuron specific enolase. There was significant decrease in brain weight in Group B compared with control. There was no significant ($p < 0.05$) change in the serum levels of serotonin, malondialdehyde, cortisol alpha feto protein the test groups compared with control. Histological studies revealed pyknotic nuclei and reduced number of neurons with Nissl substances in the treated groups. Immunohistochemical sections revealed reactive astrocytes and reduced enolase activity in the treated groups indicating neurodegeneration. Ethinyl estradiol and levonorgestrel induced neurodegenerative changes in the hippocampus, amygdala and hypothalamus in rats and may influence their functions